

**OPTOFLUIDIC MICROVISCOMETER (OMV) FOR MEASURING
ADULTERATION AND BLENDING IN FLUIDS**

BY

VENKATESWARAN PS

COLLEGE OF ENGINEERING STUDIES

(DEPARTMENT OF RESEARCH AND DEVELOPMENT)

**IN PARTIAL FULFILLMENT OF THE REQUIREMENT OF THE
DEGREE OF DOCTOR OF PHILOSOPHY**

TO



UNIVERSITY OF PETROLEUM AND ENERGY STUDIES

DEHRADUN-INDIA

JANUARY 2016

UNDER THE GUIDANCE OF

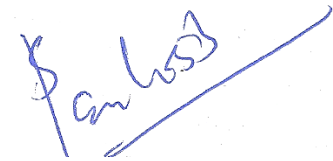
DR. SANTOSH DUBEY

DEPARTMENT OF PHYSICS

UNIVERSITY OF PETROLEUM AND ENERGY STUDIES

This is to certify that the thesis on “Optofluidic Microviscometer (OMV) for measuring Adulteration and Blending in Fluids” by Venkateswaran PS in partial completion of the requirement for the award of the degree of doctor of philosophy (engineering) is an original work carried out by him under our joint supervision and guidance.

It is certified that the work has not been submitted anywhere else for the award of any other diploma or degree of this or any other university.



DR. SANTOSH DUBEY

Asst. Professor (SG), Department of Physics, UPES-Dehradun, India



DR. SANKET GOEL

Associate Professor, EEE, BITS-Pilani, Hyderabad Campus, India



DR. AJAY AGARWAL

Senior Principal Scientist, CSIR-CEERI-Pilani, India



DR. PARAG DIWAN

Chief Academic Officer (Energy Programs), Laureate International Universities, India

ACKNOWLEDGEMENTS

First and foremost I would like to express my utmost gratitude to my advisors, Dr. Santosh Dubey and Dr. Sanket Goel for their constant support, encouragement, constructive criticism and immensely valuable suggestions throughout my PhD tenure. This doctorate would not have seen the light of the day without their invaluable ideas and creative intellectual support. My association with them has also taught me to appreciate the value of persistent tolerance in the development of healthy scientific environment.

I sincerely thank Dr. Parag Diwan for his resolute support and inspiration in taking up this research work.

I would like to thank Dr. Ajay Agarwal from CSIR-CEERI for generously helping me with my research and allowing me to work in his laboratory at Pilani.

I would like to thank Dr. Kamal Bansal for his guidance and backing in the various stages of my doctoral research.

I sincerely acknowledge the overall support and guidance of Dr. S J Chopra, Chancellor, UPES and Dr. Chandra Shekhar, Ex-Director, CSIR-CEERI, Pilani India for helping me carrying out this research project at both the organizations.

I would also like to thank the Department of Science and Technology (Government of India) for their financial support to this research project (File No. #DST/TSG/ME/2012/08).

I honorably thank all the Members of the Faculty Research Committee for their constant suggestions, advice and generous contributions from time to time.

I also thank the Members of CCE and SRE for their timely help and support in the various stages of my doctoral work.

I would like to mention the undaunted help and support from Mr. Abhishek Sharma, Assistant Professor-Electronics Engineering at UPES in helping with the conduction of experiments and analysis of data.

I am indebted to my manager Dr. Jitendra Pandey and ex-colleagues Mr. A Kartik and Mr. Diwakar Kashyap for their consistent encouragement and help.

I would like to thank Ms. Tamalika Bhakat and Mr. Mukesh Sonani, students of CSIR-CEERI, Pilani for their support in biodiesel testing.

I would also like to thank Ms. Ishita Agarwal, Mr. Manav Makin, Mr. Bhanu Gaur, Mr. Siri, Mr. Pranshu Pandey and Ms. Injila Khan of the B.Tech Material Science department of UPES for their invaluable help in the experimentation.

I profoundly thank my parents, Mr and Mrs. Sankaran for their unflinching support and my brother, Mr. PS Sriram for his invaluable backing.

Finally, I would like to gratefully acknowledge my wife, Mrs. PV Roshini, for having confidence in me and being proud at what I was at each and every moment of my life and to my little son, Mr. PV Shivnarayan for filling my life with joy and happiness.

EXECUTIVE SUMMARY

During the last few years, the dependency on alternate energy has been growing with steady pace and significance; thereby providing an abundant scope for deploying new technological solutions to growing problems like pollution, adulteration and corruption. It is a well-known fact that additives added to any liquid fuel directly affects the performance and efficiency of any automobile. The same fact applies to adulteration in common commodities like milk, curd and soft drinks. The various physical properties that govern the nature of fluids include viscosity, concentration, boiling point, melting point, etc. The additives and other adulterants produce a change in these properties. Therefore, developing a sensor based on the physical properties of such fluids can provide a reliable and effective solution for detection and monitoring of adulterants. There are a host of devices available in the market for measuring adulteration in fluids. Most of them are either complex or need a huge lab space with a trained instructor for the operation. This makes it challenging for a common man to measure adulteration at ground level.

This thesis describes the designing, fabrication, theoretical modeling and experimental validation of a 3D printed lab-on-chip microfluidic device which measures adulteration by analyzing the variations in dynamic viscosity of a fluid in a palm-sized variant without the need of an experienced operator. The working principle in this device is viscosity dependent width capture by two immiscible fluids flowing into a rectangular microchannel at the same flow rate. The theoretical model of the device has been based on the modified Hagen-Poiseuille flow equation with emphasis on flow rate, sample volume and viscosity as major parameters. The dynamic viscosity of various samples have been tested w.r.t a reference solution and the test results have been verified using a standard rheometer. The tests were conducted for three types of sample groups. The first group comprised of several blending ratios of diesel with biodiesel. The second group was a sample galore of various commonly mixed adulterants (of different ratios) in milk. The third and final group consisted of samples formed by a mixture of three conventional fuels namely petrol, diesel and kerosene. The design and fabrication of the device using the conventional micromachining and the advanced 3D printing technology has been discussed in detail. This optical microviscometer has many advantages over other devices like simple design, quick 3D fabrication, low cost, low sample volume, excellent insulation, transparency, durability and accuracy. The simple and versatile device design offers the advantage of being compatible for many other applications like food adulteration, haemoglobin detection, PT-INR measurement, etc.

TABLE OF CONTENTS

1. INTRODUCTION	9
1.1 OVERVIEW	9
1.2 LITERATURE SURVEY	11
1.2.1 REVIEW OF ADULTERATION MEASUREMENT TECHNIQUES	11
1.2.2 REVIEW OF MICROVISCOMETER TECHNIQUES..	14
1.3 OBJECTIVES.....	15
1.4 METHODOLOGY	15
1.4.1 THEORETICAL APPROACH TO THE RESEARCH PROBLEM.....	15
1.4.2 OPTICAL MICROVISCOMETER.....	20
2. FABRICATION OF THE OPTICAL MICROVISCOMETER BY CONVENTIONAL MICROMACHINING AND 3D PRINTING	22
3. MICROMACHINED OPTICAL MICROVISCOMETER FOR THE TESTING OF BIODIESEL BLENDS	28
3.1 OVERVIEW	28
3.2 DEVICE DESIGN	30
3.3 RESULTS AND DISCUSSION.....	31

4. 3D PRINTED OPTICAL MICROVISCOMETER FOR THE TESTING OF MILK ADULTERATION	34
4.1 OVERVIEW	34
4.2 DEVICE DESIGN	35
4.3 SAMPLE PREPARATION AND EXPERIMENTAL SETUP	36
4.4 RESULTS AND DISCUSSION	39
4.4.1 WATER ADULTERATION IN MILK	39
4.4.2 FLOUR ADULTERATION IN MILK	40
4.4.3 STARCH ADULTERATION IN MILK	42
4.4.4 UREA ADULTERATION IN MILK	44
5. 3D PRINTED OPTICAL MICROVISCOMETER FOR THE TESTING OF AUTOMOBILE FUEL ADULTERATION	47
5.1 OVERVIEW	47
5.2 SAMPLE PREPARATION AND EXPERIMENTAL SETUP	48
5.3 RESULTS AND DISCUSSION	51
6. CONCLUSION AND FUTURESCOPE	60
7. APPENDIX A	64
8. REFERENCES	69

LIST OF TABLES AND FIGURES

Table 5.1 Sample List of Conventional Fuels

Figure 1.1 Flow of two immiscible fluids between a pair of horizontal plates under the influence of a pressure gradient

Figure 1.2 Optical Microviscometer

Figure 2.1 Micromachined Design on an Acrylic Sheet

Figure 2.2 Bonding Issue and Leakage in a Micromachined Device

Figure 2.3 MiiCraft 3D Printer Kit

Figure 2.4 Optofluidic Microviscometer (a) Design 1 (b) Design 2

Figure 3.1 (a) The design parameter of the Microfluidic device (in mm), and (b) Acrylic Sheet showing the Device Design

Figure 3.2 Experimental Set-up for Measurement of Viscosity of the Biodiesel Samples

Figure 3.3. Interface shift between the Reference Fluid (Glycerin) and Test Fluid (Biodiesel) of varying viscosity (a) B40 and Glycerin (b) B80 and Glycerine

Figure 3.4 Percentage of Channel Fraction versus Sample Viscosity

Figure 4.1 (a) Geometry (b) 3D Printed Output of the Optofluidic Microviscometer using Rhinoceros Ver. 5.10

Figure 4.2 (a) Schematic of the Setup (b) Actual Experimental Setup

Figure 4.3 Biphasic Interface Position Measurement for Flour in Milk using the OMV

Figure 4.4 Width Occupied by Water Adulterated Milk Sample Vs Sample Viscosity

Figure 4.5 (a) Width Occupied by Flour Adulterated Milk Sample Vs Sample Viscosity

Figure 4.5 (b) Calculated and Measured Viscosity of the Flour Adulterated Milk Sample

Figure 4.6 (a) Width Occupied by Starch Adulterated Milk Sample Vs Sample Viscosity

Figure 4.6 (b) Calculated and Measured Viscosity of the Starch Adulterated Milk Sample

Figure 4.7 (a) Width Occupied by Urea Adulterated Milk Sample Vs Sample Viscosity

Figure 4.7 (b) Calculated and Measured Viscosity of the Urea Adulterated Milk Sample

Figure 5.1 (a) Width Occupied by Petrol Adulterated with Diesel Sample Vs Sample Viscosity

Figure 5.1 (b) Measured and Actual Dynamic Viscosity of Petrol Adulterated with Diesel

Figure 5.2 (a) Width Occupied by Petrol Adulterated with Kerosene Sample Vs Sample Viscosity

Figure 5.2 (b) Measured and Actual Dynamic Viscosity of Petrol Adulterated with Kerosene

Figure 5.3 (a) Width Occupied by Diesel Adulterated with Kerosene Sample Vs Sample Viscosity

Figure 5.3 (b) Measured and Actual Dynamic Viscosity of Diesel Adulterated with Kerosene

Figure 5.4 (a) Width Occupied by Petrol Adulterated with Diesel and Kerosene Vs Sample Viscosity

Figure 5.4 (b) Measured and Actual Dynamic Viscosity of Petrol Adulterated with Diesel and Kerosene

Figure 6.1 (a) Electronic Microviscometer Concept (b) 3D Printed Device

Figure 7.1 Volume Element inside a Micro-channel

Figure 7.2 Positioning of the Volume Element in the Channel

CHAPTER I

1. INTRODUCTION

1.1 OVERVIEW

Adulteration has become a major issue of concern in the recent years. Many things purchased from the market are found to be either fake or a mixture of a number of adulterants. We find majority of the adulteration in liquid commodities as they are more prone to this act of corruption. The two major grey areas are fuel and milk. In developing countries, it is always a challenge to detect and monitor the adulteration of fuel or milk. This adulteration of fuel has potential side-effects on the engines and the environment. Whereas the adulteration of milk has serious health related issues. India in comparison to other countries faces a lot of problems with fuel and milk adulteration and must seriously work towards realizing a simple, user friendly method to detect and monitor this at the household level [1, 2]. The system must be easily deployable-and-pluggable, robust, user and equipment friendly, in situ, inexpensive and trustworthy method to monitor the composition. For this, on the technology front, we need to use one or a few of the physio-chemical properties which directly affect the functioning of such liquids. Such a device should potentially be integrated into a system which can display the adulteration along with other functionalities.

Viscosity is an important rheological property that can be defined as resistance to fluid flow [3]. In simple terms, viscosity is the thickness or the internal resistance between layers of the flowing fluid. Viscosity measurement is of great importance both in research and industrial applications [3-8]. A viscometer is a measuring instrument which is used to measure the viscosity of the fluid whose surroundings

are constant throughout the experiment. A rheometer is a device that is used to measure the viscosity of those fluids whose viscosity varies under different conditions like pressure, temperature, etc. [9, 10].

Although commercial rheometers and viscometers are available but due to their obvious limitations, such as, being lab-based, expensive, not providing real-time results, need of lot of sample volume, these systems may not be suitable to detect and monitor as per the user's requirement. A lab-on-a-chip or micro-fluidics based microviscometer, will not only be able to tackle such limitations but also lead to provide a miniaturized micro-total-analysis-system to work as a sample-to-answer real-time system.

Microfluidics have emerged as a promising technology for a wide range of applications from micro-chemistry to bio-engineering[11]. It provides a pathway to address many issues related to the dimensions of devices and miniaturized sensors for various applications. Microfluidic devices offer several advantages over large scale processes such as small sample requirement, improved analysis time, real time monitoring, and high aspect ratio etc.[12-14]. The usage of microviscometer to do the viscosity testing has been in research for quite some time[15]. Leveraging well-proven micro-fabrication technology, this thesis describes the design, fabrication and testing of a LOC device and its use in detecting dynamic viscosities of various fluids. Moreover this device can easily be used to detect any sample with viscosity as the physical property for measurement. Being the central property in a micro fluidic environment, the viscosity and its variation can directly be observed and analyzed using LOC devices. Moreover, in comparison with the conventional viscometers, the microviscometer can be fabricated easily in a simple clean- room, is prone to be inexpensive on mass-production, can be integrated with the existing microcontrollers in the automobiles and able to sense even a small adulteration ratio [16]. In summary, the research work in this thesis is an attempt to provide a solution to the challenge to implement a micro-device for various biochemical

applications to be in-line with the proposed Energy thrust areas in the 12th five-year plan of the Government of India, and will play a major role in providing a viable solution towards the climate change initiatives [17]. This microviscometer has been used to detect the change in dynamic viscosity for various biodiesel blends and to measure the adulteration in milk and automobile fuels [18, 19].

1.2 LITERATURE SURVEY

1.2.1 REVIEW OF ADULTERATION MEASUREMENT TECHNIQUES

In India, several regulatory policy and legal frameworks have been adopted and practiced to find, control and curb adulteration in liquids [20]. Some of these tests are based on determining physio-chemical properties while others are based on measuring the impact of these liquids in various applications and environments [21]. Tests based on different physio-chemical properties that have been used to measure adulteration are as follows -

Density test (ASTM D4052) [22] utilizes hydrometer and densitometer to determine the sample density. Although this method provides very good accuracy, but it has several disadvantages, such as, huge set-up cost, requirement of a controlled environment (not feasible to use in-field) and requirement of low-precision. Gas Chromatography (GC) [23] has been harnessed to detect adulterants in samples. However it requires an experienced technician to operate the equipment and interpret the results. It is an effective method for detection of adulterants in various sources but it would require substantial lab space, specific sample preparation and an experienced operator.

Evaporation Test (ASTM D3810) [24] has been used to detect low concentrations of kerosene (5%) in gasoline and of diesel (1-2%) in gasoline using filter-papers. Distillation Test (ASTM D86) [23] uses the boiling points difference of adulterated liquid samples. This technique is also not suitable for field use due to the bulkiness of the equipment and the process being time consuming.

On the technology front, there has been rigorous work on developing specifically designed methods, based on physio-chemical properties of liquids for adulteration measurement. Following few efforts have been made in India -

Gupta and Sharma [21] proposed a method using sound/ultrasound sensor, which is based on the validated assumption to measure the change in speed of sound in a fluid, to detect/estimate the volume percentage of commonly used adulterants in automobile fuel. Here, the authors concluded that it is feasible to develop an easy to operate equipment which measures and uses the measured speed of sound to estimate the adulterants in fuel.

Roy [25] proposed a fiber-optic sensor using an unclad fiber to measure the adulterated fuel by observing the change in the index of refraction. Vandana et al [26] leveraged the long-period optical fiber gratings (LPOFG) based sensor for monitoring the adulteration in fuels. Both these methods were demonstrated to measure the concentration change up to 1% for kerosene in petrol and diesel. The methods based on fiber-optics are expensive with requirements for bulky equipment's and are primarily lab-based.

While the above mentioned conventional tests (Density, Chromatography, Evaporation and Distillation) have widely been implemented internationally, few specifically designed methods have been reported to measure and monitor adulteration in liquids.

Li et al [27] designed gas sensors based on the change in electrical dc resistance (or ac impedance) upon exposure to volatile compounds. They are known as chemo-resistive sensors and consist of thin (1 – 50 μm) doped polymer films deposited onto inter-digitated electrodes by circuit printing. The system was used to detect and discriminate many different types of volatile organic compounds often present in polluted indoor air. These sensors are inexpensive (US\$1), can be operated at room temperature with low power consumption (<1mW) and are insensitive to humidity.

Benvenho et al [28] developed a similar chemo-resistive sensor that is insensitive to gasoline but quite sensitive to ethanol. This work shows a linear relative response for gasoline/ethanol blend ranging from 5% onwards.

Li et al [29] presented a gas sensor based on capacitive sensing technique to study organic volatile substances. The chemo-capacitor is based on the change of capacitance caused by the change in dielectric constant, due the modifications in polarization properties of molecules and/or atoms inside the active layer by external perturbations. The authors used nano-porous silicon as an active layer between inter-digitated electrodes and observed a non-linear increase of the capacitance when the concentration of ethanol in air was increased. Extending this work, Wiziack et al. [30] used an array of eight capacitive polymeric sensors to discriminate gasoline, diesel, ethanol and some common fuel adulterants as toluene, hexane and water. These results depend on the polymeric material used as active layer and their interaction with organic volatile compounds.

Although many of these methods have high accuracy, most of these methods cannot be deployed for on-field operation. This is due to heavy one-time test cost, need of a controlled environment, need of a dedicated or experienced operator, expensive testing-and-measurement equipment and ex-situ operation.

1.2.2 REVIEW OF MICROVISCOMETER TECHNIQUES

Some work has been carried out to conceptualize, design, fabricate and test a microviscometer. A range of materials, such as silicon [30], glass [31, 32] and different polymers (SU-8 and PDMS) [33-35] have been used to realize a microviscometer.

Srivastava et al [31] described a silicon based fully automated method working on droplet sensing technique using a single layer of metal lines to micro-fabricate and produce electronic signal using low DC voltages. Droplets as small as 100 pL were detected and the system was automated to sense range of viscosities. The viscometer is completely controlled by a laptop computer, and the total time for operation including setup, calibration, sample addition and viscosity calculation is approximately 4 minutes.

Lee et al [32] described a microchip method to measure polymer and biopolymer solutions. After diluting the polymer samples with solvent in the micro-fluidic chip, the concentration and flow dilutions of the polymer sample were calculated from the fluorescent signals recorded over a range of dilutions. The viscosities at various polymer dilutions were evaluated using mass and momentum balances in the pressure-driven micro-channel. This technique is suitable to observe conformation changes in biological samples, but may not suit the hydrocarbons and other household liquid commodities.

Chevalier and Ayela [33] presented a micro-machined capillary on chip rheometer using anodically bonded silicon-pyrex derivative microchannels equipped with local probes, and used silicon oil and ethanol-based nano-fluids. With this device, the local pressure drop was measured inside the microchannels dielectro-phoretically without the need of reference fluid.

Han et al [34, 35] demonstrated a poly (dimethylsiloxane) (PDMS) micro-fluidic device for measuring the viscosity of Newtonian fluids by using the high solubility and permeability of air in PDMS to generate vacuum (and get pressure differential) in the degassed PDMS micro- fluidic device. This device was used for different types of samples, such as, glycerol, proteins, blood plasma and organic solvents.

1.3 OBJECTIVES

- To model two immiscible fluids flowing in a rectangular micro-channel and to draft the design parameters for fabrication of the microviscometer
- To fabricate micro-fluidic device (microviscometer) for detection and monitoring of bio-fuel blending, milk adulteration and conventional fuel adulteration
- Design a robust and simple model using Rhino software
- Perform micromachining and stereo lithography followed by etching to generate the final model
- Generate multiple prototypes of the device using the 3D printer
- Test the flow patterns and analyze the device limitations
- Characterize the micro-chips using different fluids with known viscosities
- Troubleshooting and testing of the microviscometer in a suitable viscosity range
- Generate samples in various ratios of adulterations with known adulterants
- Find the viscosity of different samples and compare with known viscosities and analyze the efficiency of the device

1.4 METHODOLOGY

1.4.1 THEORETICAL APPROACH TO THE RESEARCH PROBLEM

Flow of Two Adjacent Immiscible Liquids in a Horizontal Channel

Based on the derivation performed by Bird et al [36] for the flow of two immiscible fluids in a rectangular channel, we have also considered two immiscible fluids flowing in a rectangular channel of length L and width W under the influence of a horizontal pressure gradient $\frac{P_0 - P_L}{L}$. Our derivation, however, is different than the one performed by Bird et al in the sense that we have fixed the flow rates of the fluids at the input and estimate the width occupied by both the fluids as they flow along the channel, whereas Bird et al adjusted the flow rates at the input such that the width occupied by both the fluids is same in the channel. The velocity profile of both the immiscible fluids in a rectangular channel has been displayed schematically in figure 1.1. In this figure, we see that both the fluids have different velocity profiles across the interface; the velocity at the interface is the same. The width occupied by both the fluids has been also different, which we found experimentally.

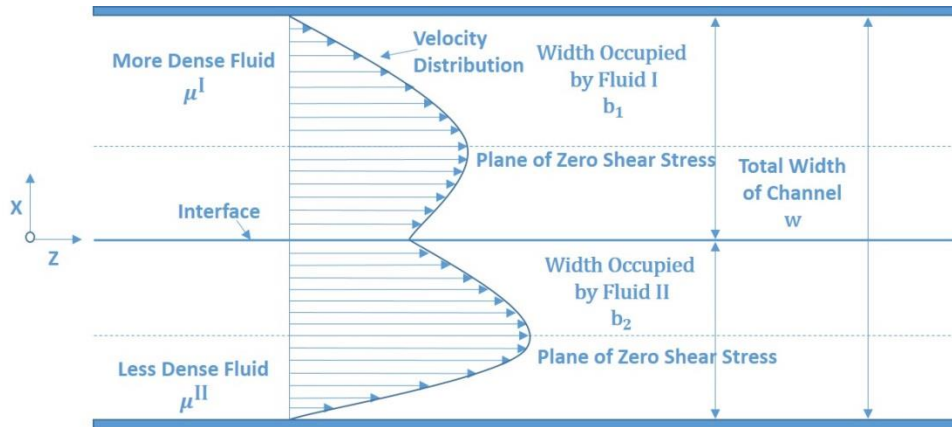


Figure 1.1: Flow of two immiscible fluids between a pair of horizontal plates under the influence of a pressure gradient

The differential equation for the momentum-flux could be written:

$$\frac{d\tau_{xz}}{dx} = \frac{P_0 - P_L}{L} \quad (1)$$

Integration of eq. (1) for the two fluids flowing in and occupying specific regions in the channel leads to

$$\tau_{xz}^I = \left(\frac{P_0 - P_L}{L} \right) x + C_1^I \quad (2)$$

$$\tau_{xz}^{II} = \left(\frac{P_0 - P_L}{L} \right) x + C_1^{II} \quad (3)$$

The momentum flux is considered to be continuous throughout the fluid-fluid interface; hence applying this as a boundary condition, we get:

$$\text{B.C. 1:} \quad \text{at } x = 0, \tau_{xz}^I = \tau_{xz}^{II}$$

Therefore $C_1^I = C_1^{II} = C_1$. Equations 2 & 3 become:

$$-\mu^I \frac{dv_z^I}{dx} = \left(\frac{P_0 - P_L}{L} \right) x + C_1 \quad (4)$$

$$-\mu^{II} \frac{dv_z^{II}}{dx} = \left(\frac{P_0 - P_L}{L} \right) x + C_1 \quad (5)$$

The above two equations can be integrated to obtain the velocity equations for the two fluids:

$$v_z^I = - \left(\frac{P_0 - P_L}{2\mu^I L} \right) x^2 - \frac{C_1}{\mu^I} x + C_2^I \quad (6)$$

$$v_z^{II} = - \left(\frac{P_0 - P_L}{2\mu^{II} L} \right) x^2 - \frac{C_1}{\mu^{II}} x + C_2^{II} \quad (7)$$

Using the fact that the velocity of both the fluids at the interface is equal and the conditions for no-slip at both the boundaries along x -direction, the integration constants may be estimated:

$$\text{B.C. 2:} \quad \text{at } x = 0, \quad v_z^I = v_z^{II}$$

$$\text{B.C. 3:} \quad \text{at } x = b_1, \quad v_z^I = 0$$

$$\text{B.C. 4:} \quad \text{at } x = -b_2, \quad v_z^{II} = 0$$

Applying the boundary conditions in equations 6 & 7, we get:

$$C_2^I = C_2^{II} \quad (8)$$

$$0 = -\left(\frac{P_0 - P_L}{2\mu^I L}\right) b_1^2 + \frac{C_1}{\mu^I} b_1 + C_2^I \quad (9)$$

$$0 = -\left(\frac{P_0 - P_L}{2\mu^{II} L}\right) b_2^2 - \frac{C_1}{\mu^I} b_2 + C_2^{II} \quad (10)$$

From these three equations we get

$$C_1 = \left(\frac{P_0 - P_L}{2L}\right) \left(\frac{\mu^{II} b_1^2 - \mu^I b_2^2}{\mu^{II} b_1 + \mu^I b_2}\right) \quad (11)$$

$$C_2^I = C_2^{II} = \left(\frac{P_0 - P_L}{2L}\right) \left[\frac{b_1 b_2 (b_1 + b_2)}{\mu^{II} b_1 + \mu^I b_2}\right] \quad (12)$$

The resulting velocity profiles would be:

$$v_z^I = -\left(\frac{P_0 - P_L}{2\mu^I L}\right) x^2 - \frac{x}{\mu^I} \left[\left(\frac{P_0 - P_L}{2L}\right) \left(\frac{\mu^{II} b_1^2 - \mu^I b_2^2}{\mu^{II} b_1 + \mu^I b_2}\right) \right] + \left[\left(\frac{P_0 - P_L}{2L}\right) \left(\frac{b_1 b_2 (b_1 + b_2)}{\mu^{II} b_1 + \mu^I b_2}\right) \right] \quad (13)$$

$$v_z^{II} = -\left(\frac{P_0 - P_L}{2\mu^{II} L}\right) x^2 - \frac{x}{\mu^{II}} \left[\left(\frac{P_0 - P_L}{2L}\right) \left(\frac{\mu^{II} b_1^2 - \mu^I b_2^2}{\mu^{II} b_1 + \mu^I b_2}\right) \right] + \left[\left(\frac{P_0 - P_L}{2L}\right) \left(\frac{b_1 b_2 (b_1 + b_2)}{\mu^{II} b_1 + \mu^I b_2}\right) \right] \quad (14)$$

Upon double differentiation we get

$$\frac{d^2 v_z^I}{dx^2} = -\left(\frac{P_0 - P_L}{\mu^I L}\right) \quad (15)$$

$$\frac{d^2 v_z^{II}}{dx^2} = -\left(\frac{P_0 - P_L}{\mu^{II} L}\right) \quad (16)$$

From both the equations, we see that:

$$\frac{(P_0 - P_L)}{L} = \mu^I \frac{d^2 v_z^I}{dx^2} = \mu^{II} \frac{d^2 v_z^{II}}{dx^2} \quad (17)$$

According to Hagen-Poiseuille's law for laminar flow in a rectangular channel [37]:

$$Q = \frac{\Delta P b h^3}{12 L \mu} \quad (18)$$

Here

ΔP is the pressure difference between inlet and outlet

b is the width occupied by the fluid in the channel

h is the height of the channel

μ is the viscosity of the fluid

L is the length of the channel

In the case of two immiscible fluids flowing in the same channel, the flow rates can be written as

$$Q^I = \frac{\Delta P^I b_1 h^3}{12 \mu^I L} \quad (19)$$

$$Q^{II} = \frac{\Delta P^{II} b_2 h^3}{12 \mu^{II} L} \quad (20)$$

If the flow rates are adjusted to be the same for both the fluids, then

$$\frac{\Delta P^I b_1 h^3}{12 \mu^I L} = \frac{\Delta P^{II} b_2 h^3}{12 \mu^{II} L} \quad (21)$$

Equation 21 may be further simplified as:

$$\frac{\Delta P^I b_1}{L \mu^I} = \frac{\Delta P^{II} b_2}{L \mu^{II}} \quad (22)$$

We know that

$$\frac{\Delta P}{L} = \mu \frac{d^2 v_z}{dx^2} \quad (23)$$

[Refer Appendix A (Chapter 7) for the source]

Replacing $\Delta P/L$ in equation 22 with the help of equation 23 we get:

$$\mu^I \frac{d^2 v_z^I}{dx^2} \frac{b_1}{\mu^I} = \mu^{II} \frac{d^2 v_z^{II}}{dx^2} \frac{b_2}{\mu^{II}}$$

Using equation 17, we get

$$\frac{b_1}{\mu^I} = \frac{b_2}{\mu^{II}}$$

Which may be rearranged as

$$\frac{\mu^I}{\mu^{II}} = \frac{b_1}{b_2} \quad (24)$$

Therefore, the viscosities of two immiscible fluids flowing inside a horizontal channel (of height h) and occupying widths b_1 and b_2 respectively, will be related by equation 24.

1.4.2 OPTICAL MICROVISCOMETER

In the optical microfluidic device with Y-shape channel as shown in the figure 1.3, there are two flow-streams arriving from two side channels and mixing into the main channel. For both the flow-streams, all the parameters of the modified Hagen-Poiseuille flow equation remains the same except the width occupied by the individual flow-streams in the main channel.

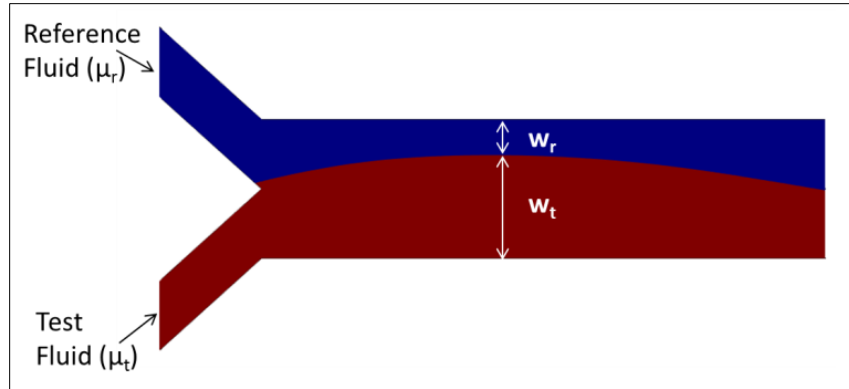


Figure 1.2 Optical Microviscometer

Once we know the ratio of the widths occupied by the fluids and the viscosity of the reference fluid, we can calculate the viscosity of the test fluid. The design parameters for such an optical device could be as follows

Parameter	Range
Channel Width	0.5 mm to 1 mm
Channel Depth	0.5 mm to 1 mm
Main section length	2.5 mm
Angle between two Y sections	10^0 to 20^0
Material	UV Curable Acrylic Polymer

CHAPTER II

2. FABRICATION OF THE OPTICAL MICROVISCOMETER BY CONVENTIONAL MICROMACHINING AND 3D PRINTING

Microfluidics requires design parameters to be in the order of microns and one of the easiest routes for realizing components at that scale was a well-known CNC (Computer Numerical Control) router for micromachining. The material and tool size limitation in micromachining made it difficult to realize a device made of acrylic and in the size order of 50 microns. The initial idea was to get it done using the carving machines in the interior design plants but then it became increasingly difficult as the usage of a particularly small sized tool was needed. This process also hampered the manufacturing of other products which made it more difficult. This made other routes of fabrication to be explored rigorously. One such method was to use the machine and the micron sized tool of a local badge manufacturer near the Indian Military Academy of Dehradun. The results

obtained were accurate to the scale of few hundreds of microns as shown in the figure 2.1.

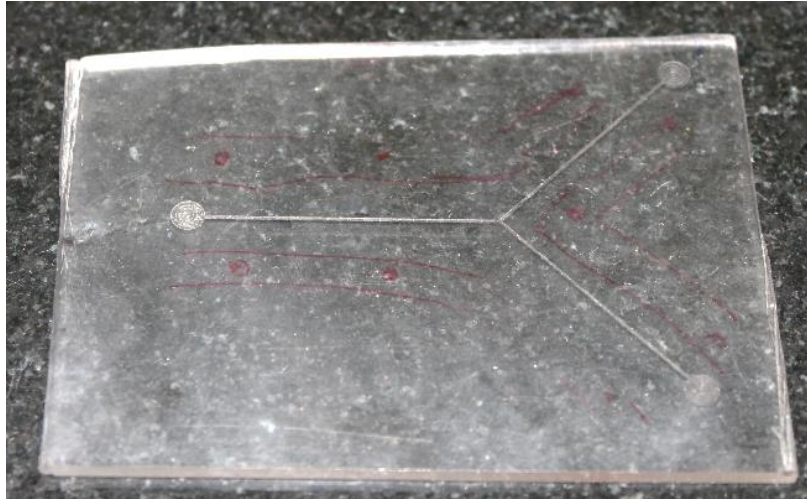


Figure 2.1 Micromachined Design on an Acrylic Sheet

For the above shown design, the micromachining was to be done on one plate and a second plate needed to be bonded to the first for a leak-proof device. But during the bonding and sealing process which is done manually, either the alignment failed or the positioning of the sheet shifted. Besides, the bond was not strong enough to stop the leakage of fluid into the sides of the actual channel thereby hampering the measurement as shown in the figure 2.2.

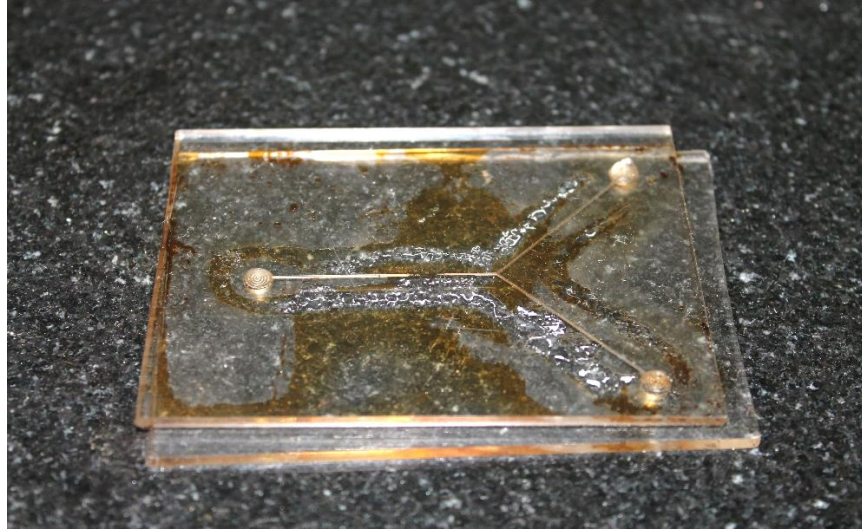


Figure 2.2 Bonding Issue and Leakage in a Micromachined Device

However, in microfluidics the most important parameter is the size followed by the steady flow of the fluid in the channel. In order to make the fluid flow in micro-channels, it is an absolute necessity to supply a pressure differential. These parameters caused problems while performing the experiments. With the advent of rapid prototyping combined with the limitless possibilities of 3D printing, the problems associated with the micromachining could be resolved. The applications of rapid manufacturing technology is useful for various functions ranging from biological studies to various aspects of energy, electronics, chemistry and life sciences.

3D printing encompasses a wide spectrum of techniques, some of which are even being used in industries. But for microfluidics, one particular technique namely ‘stereolithography’ (SLA) is the one that is extensively used [38]. This is because some of the SLA based printers can go up to a resolution of 56 microns like the MiiCraft 3D printer. This method provides us with the flexibility of printing complex three dimensional structures using polymeric materials [39]. The major hurdle of using external pumps and pumping equipment was solved by Begolo and his team by 3D printing the disposable parts (pumping lid and cup) of the

pumping mechanism in a microfluidic system and placing them before the channel inlet to send in the fluid by pressing the lid for pressure [40].

Many components pertaining to microfluidics like optical and electronic devices (base design), valves, mixers and even infusion pumps can be fabricated using the rapid prototyping techniques like laser ablation, PDMS casting, nanoimprinting and 3D printing [41]. The device printed by such quick processing methods are often called in as disposable devices, reason being that they take very less time to be fabricated combined with low cost material and fabrication technique [42]. Microfluidics being an area where the sample volume requirement is very less combined with the small size of the integrated system and the lesser time need for measurement enabling it to be the most preferred analysis and diagnostic technique in the biomedical world. Complex features and integration of such features is the real challenge in microfluidics [43-45]. Many research groups work on the 3D model designing of complex features involving membranes and varying channel sizes which can enable the study of drug transport to the diseased cells [46]. Such micro-total-analysis systems can at a single time carry out parallel processing of many tasks to churn out the required outputs [47].

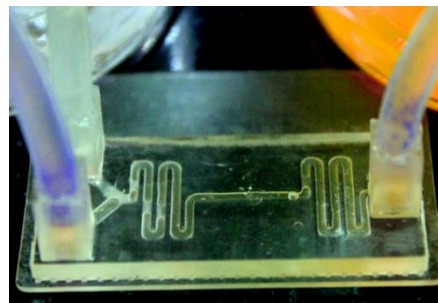


Figure 2.3 MiiCraft 3D Printer Kit

The 3D printer used in this research to print the optical microviscometer was MiiCraft Kit (PN#95.LF800G004) from the Rays Optics, Taiwan shown in the figure 2.3. This is a stereo-lithography (SLA) based printing machine with a minimum resolution of 56 microns across the XY axis and 50 microns across the Z axis. It uses the bottom-up approach of printing based on UV resin curing technique [48].



(a)



(b)

Figure 2.4 Optofluidic Microviscometer (a) Design 1 (b) Design 2

The output file from the design software should essentially be saved in the STL format for the MiiCraft STL Viewer to position the design on the platform of the printer. This is followed by the Slicer program which slices the entire design into

50 micron individual slices and generates the final index file for printing in the 'Print STL Model' module. The printer usually takes less than 5 minutes to print a model of height 1 mm using a standard available UV curable polymer input material. And after the printing it usually goes into a 5 minute post-curing cycle for the final product as shown in the figure 2.4 (a) and (b). The input material used is a transparent resin (MA-YG2005T) supplied by the company. It is a transparent liquid having a flash point of 150⁰C and a specific gravity of 1 gm/ml at 25⁰C.

CHAPTER III

3. MICROMACHINED OPTICAL MICROVISCOMETER FOR THE TESTING OF BIODIESEL BLENDS

3.1 OVERVIEW

Alternate energy has come a long way since its gain in importance due to the depleting fossil fuel reserves and the need to conserve global resources for the future generations[49]. The usage of alternate fuels in automobiles mark a significant progress in this field enabling the reduction of emissions and also supporting the cause of depleting resources[50]. Biofuels are of many types ranging from ethanol or methanol based ones to the blended ones where certain quantity of biofuel is mixed with the existing fuels such as diesel and petrol[51]. Biodiesel is an alternative for diesel. It can be obtained by trans-esterification of vegetable oils that are largely composed of tri-glycerols[52, 53]. The non-edible oil plants like Jatropha, Karanja, and Putranjiva etc. are used for the production of biodiesel as they are found to be very economical[54]. The emissions such as smoke, CO, and other particulates of the combustion process for producing the energy in the engines that use biodiesels are lesser than the conventional fuel based engines[55, 56]. This has a lower impact on the environment and living organisms[57].

The blending of biofuels is an important function because the level of blend determines the advancement in engine research [52]. It was initially difficult to exactly specify the percentage of biodiesel that could be blended with diesel because of the co-related factor with the uncertainty of the availability of biodiesel in the initial stages [11]. The Ministry of New and Renewable Energy-Government of India has proposed 20% blending of biofuels as a mandatory measure for both biodiesel and bio-ethanol by the end of 2017 [58, 59]. Biodiesel

usage has several advantages over conventional fuels like reduced emissions, improved combustion and high biodegradability[60, 61]. The increase in viscosity of biodiesel w.r.t to the slight variation in the production method makes this a very complicated proposition [62] as it would directly affect the engine performance and durability. The present day engines are expected to be modified to use not more than 20% blended biodiesel. Fractions more than that requires a redesigned injector which works in higher viscosity ranges [8, 63].

The blended amount of bio-fuel in diesel can be monitored by measuring the viscosity. There are some standard laboratory viscometers which are used to measure the viscosity of fluids. Most commonly used viscometers are U-shape glass viscometer, rotational and vibrational viscometer[64]. The major limitations of these viscometers are that they require large sample amounts, controlled surroundings and expensive instrumentation for measurements[9].

The viscosity of biodiesel is slightly greater than petro diesel but less than that of parent vegetable oil or fats [6, 62, 65, 66]. There is a misconception that density is directly related to viscosity but equally dense substance may have a wide range of viscosities. The conductivity of a fuel is the measure of the ability of the fuel to dissipate static electric charges because in low conductive fuel, electric charges accumulate and lead to dissipation in the form of sparks. Blends of biodiesel at or above 20% level would not require any kind of static dissipater due to increase in biodiesel conductivity (electrical conductivity of Biodiesel).

Most commonly used viscometers for the testing of fuel blends are U-shape glass viscometer, Rotational and vibrational viscometer [64]. U-shaped viscometer measures the viscosity of the fluid with known density of the fluid. The major limitations of these viscometers are that they require large sample amount and temperature bath is needed to maintain constant temperature environment. Moreover, different kinds of sensors are needed to measure the meniscus passage.

In this chapter, we report a micromachined lab-on-a-chip microfluidic device [67] that can be used to know the biodiesel blending ratio in diesel, in real-time by way of monitoring their viscosity [68]. The device records the interface position of the blended fuel and the immiscible reference fluid in a common channel. This miniaturized viscometer was made using acrylic [69]. The blending of diesel with bio-diesel was tested using this device for different blend ratios.

3.2 DEVICE DESIGN

The device was made of acrylic and the size of the device was as shown in the figure 3.1 (a). The markings were made in one sheet and then the holes for the inputs and output were made in another sheet as shown in the figure 3.1 (b).

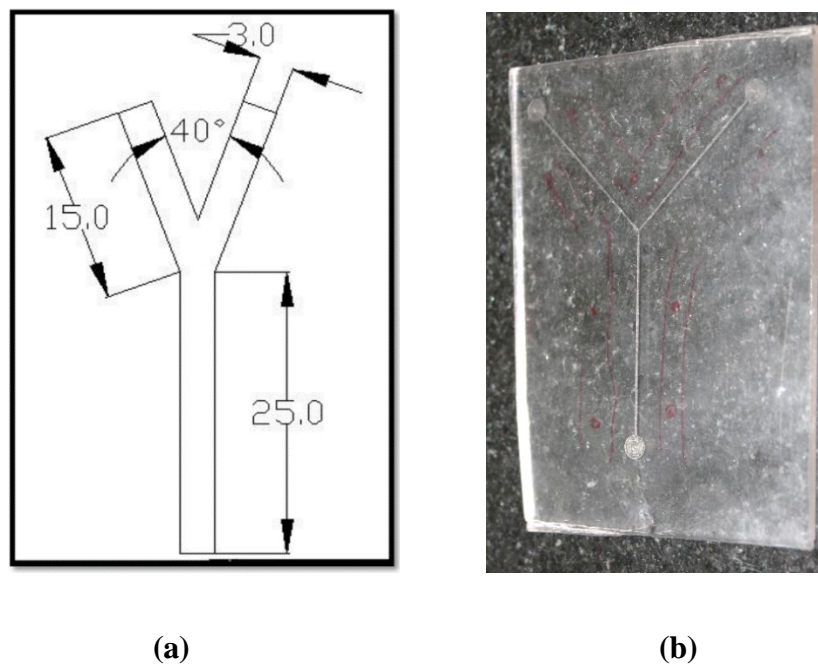


Figure 3.1 (a) The design parameter of the Microfluidic device (in mm), and (b) Acrylic Sheet showing the Device Design

Both these sheets were joined using trichloroethylene and the tubes were inserted accordingly. For biodiesel testing, glycerin was taken as reference fluid. Experimentation involved the use of two syringe pumps or infusion pumps for

pushing the fluids into the device [70]. These syringe pumps provide constant flow of two fluids throughout the channel at constant flow rate. The flow rate of two fluids was set to be same as 1ml/min. The experimental set up used for biodiesel blending analysis is shown in figure 3.2. The basic idea was to introduce two immiscible liquids through the two inputs channels and observe the interface in the common channel. When two fluids flowing through the channel have different viscosities, the more viscous fluid will have higher resistance than the other fluid. The less viscous counter-part will have better flow dynamics and hence it will take the wider path initially. But after a few minutes, stabilization occurs and it was found that the higher viscous liquid takes the wider path [71].

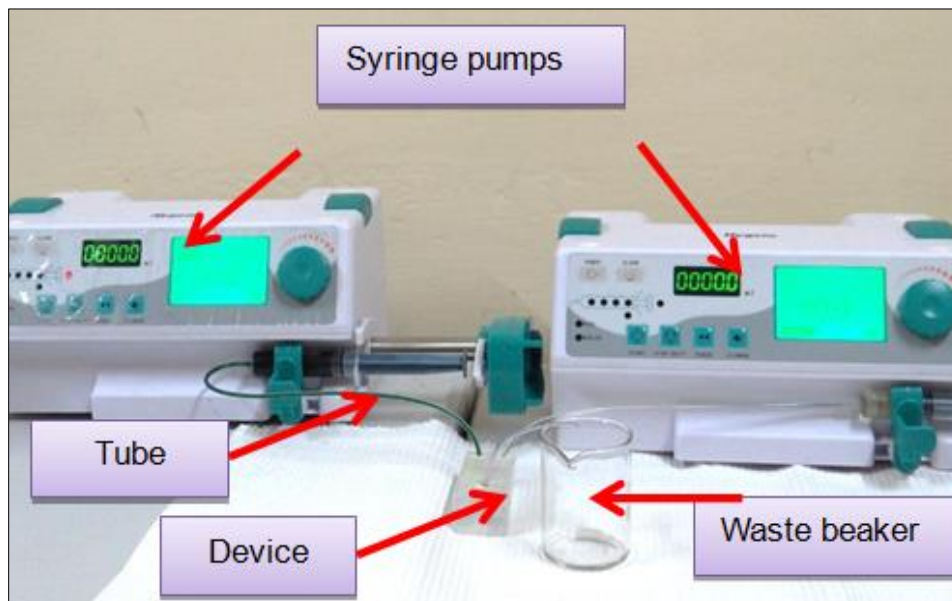


Figure 3.2 Experimental Set-up for Measurement of Viscosity of the Biodiesel Samples

3.3 RESULTS AND DISCUSSION

As shown in figure 3.3, the comparison of the theoretical model and experimental results clearly show that as the test sample of different viscosity is selected there is an interface shift i.e. the test sample with higher viscosity tends to take broader path in the common channel thereby pushing the less viscous reference fluid [72,

73]. The results were verified for various Bio-diesel blends with Glycerin as the reference fluid. Tests were also conducted with other oils including the hair oils, lubricants etc. with different densities and miscibility factor to confirm the interface shifting phenomenon [74]. Interface spreading for different oils was compared at a specific position in the channel to ensure the systematic and reliable measurements [75].

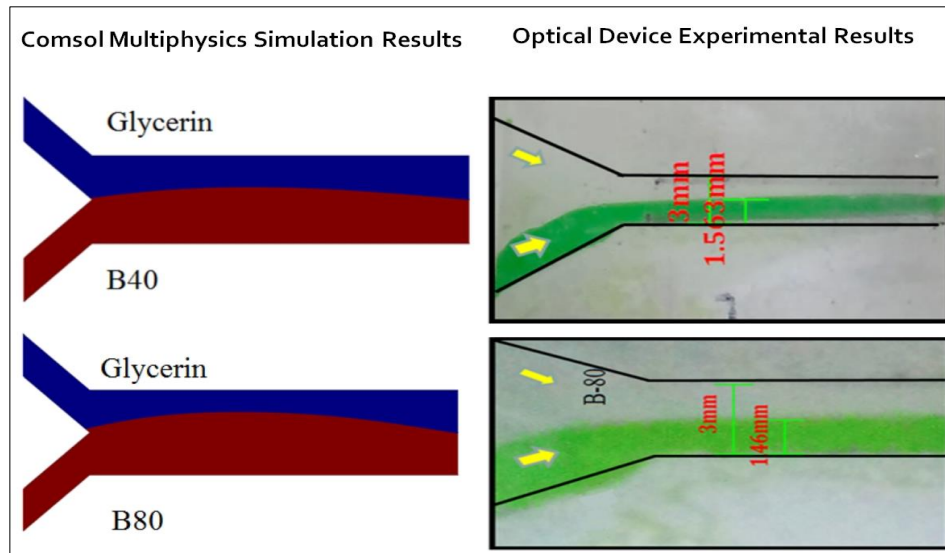


Figure 3.3. Interface shift between the Reference Fluid (Glycerin) and Test Fluid (Biodiesel) of varying viscosity (a) B40 and Glycerin (b) B80 and Glycerin

All the experiments were carried out at room temperature (25°C). Ten sets of readings for each of the blended samples with the interface position was measured using the internal software of the Leica microscope [57]. The graph was plotted between percentage of channel fraction taken up by the blended biodiesel and biodiesel viscosity [10]. This graph is then taken as a calibration curve for measuring the viscosity of unknown fuel samples. This viscosity can be used to indicate the fraction of bio-diesel in the fuel sample. Taking curve in figure 3.4 as standard graph and by using the best fit equation, the viscosity of other biodiesel samples was calculated. The percentage channel fraction occupied by the unknown sample of blended biodiesel was very close to the best fit curve.

$$y = 0.009e^{0.145x} \quad (25)$$

where, x is % of channel fraction taken by diesel/biodiesel and y is the biodiesel viscosity. By substituting the value of x in the above equation, the respective viscosity was calculated.

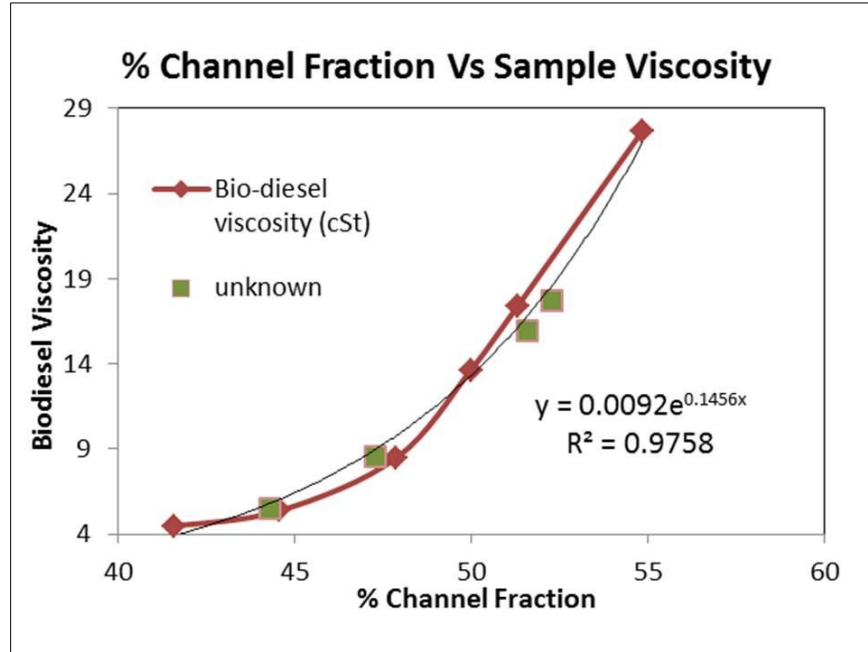


Figure 3.4 Percentage of Channel Fraction versus Sample Viscosity

This study provides a novel method of calculating viscosity of test samples on a simple microfluidic device for biofuel blending. According to the width taken by the test sample in the viscometer one can easily calculate its respective viscosity by putting the width value in the standard equation. Moreover the device is made with Acrylic and sealed using trichloroethylene at room temperature which counts for its low cost. The experimental processes have been optimized for efficient viscosity analysis for various bio-diesel blending ratios.

CHAPTER IV

4. 3D PRINTED OPTICAL MICROVISCOMETER FOR THE TESTING OF MILK ADULTERATION

4.1 OVERVIEW

Milk is the next highest consumed liquid commodity after water in the world. But to some it is a trade which reaps rich dividends [76]. Majority of the milk supply in India depends on the individual units set up by the dairy farmers in the various states of India as it is important for sustaining the livelihoods of many smallholder farmers who contribute to nearly 70 % of the total milk production in the country [77]. They go about supplying the milk to the bigger factory setups for processing and final distribution. This makes them an integral part of the process chain of milk production and distribution. In this case the profit margin scored by the individual milk producer remains constant and increases marginally state-wise based on various parameters as put forward by the Department of Animal Husbandry, Dairying & Fisheries Ministry of Agriculture-Government of India [78]. Hence, these individual producers tend to go by distributing their produce on their own. This is where the pervert problem of adulteration exists [79-81]. Most of these milk suppliers tend to play around with the viscosity of the milk that they supply in order to increase the quantity and thereby reap profits in a small scale manner. This small scale corruption results in a chain reaction when we take into account the mass of such milkmen reaping such benefits. The adulterants range from water, starch, corn-flour to urea and various detergents. Though the adulteration level is meagre, they reap better paybacks compared to that provided by companies at the cost of the consumer's health and safety [82, 83]. Hence, there is a need of a device to measure the adulteration of milk on the field.

Amongst the various available devices to test the purity of milk, the major problem exists with the size, accuracy and cost of the device. Historically, various

tests that can be performed to test the purity and quality of milk include organoleptic test, clot on boiling test, acidity test, resazurin test, conductance test and the Gerber Butterfat test [84-87]. All these tests require complex measurement, costly equipment, lot of time and an experienced operator. The major hurdle in most of them is that a common man cannot use them on a daily basis to test the milk that they receive. Besides, the parameters used to test are more complex for basic understanding. But, if one can carefully calculate and do some basic analysis, it is modest to determine that viscosity forms one of the most important parameters in the testing of milk adulteration [3, 88, 89].

The prime aim of this chapter is to explain the design and experimental analysis of a 3D printed optofluidic microviscometer that can measure the variation in the dynamic viscosity using the modified Hagen-Poiseuille flow equation of an unknown sample when it is made to flow alongside an immiscible fluid of a known viscosity. The device records the interface position of the adulterated milk sample and the immiscible reference fluid glycerin in a common channel. This microviscometer offers many advantages like better accuracy, lower cost, real-time measurement, portable and easily operated device compared to the commercially available counter-parts [69, 75, 90-92]. The meek and handy device design makes it compatible for many other applications as well. The adulteration of milk with various commonly available adulterants at different ratios of adulteration was tested in the laboratory and the analysis is discussed in the sections below.

4.2 DEVICE DESIGN

In a typical 3D printed device, the width of the channels was kept at 1 mm overall (in X, Y and Z planes) and the diameter of the inlet and outlet ports was 2.6 mm. The length and breadth of the device was fixed to 4 cm x 2.5 cm based on the maximum printable area of the 3D printer. Besides, for the analysis and measurement, this dimension was more than sufficient as the number of extended

loops helped in the proper laminar flow in the channel. The length of the lopped channels was chosen to be as long as possible within the printable area of the printer. This was done in order to make the flow of the liquids to be smooth in nature. The length of the main channel was kept as 27.5 mm as shown in the Figure 4.1(a).

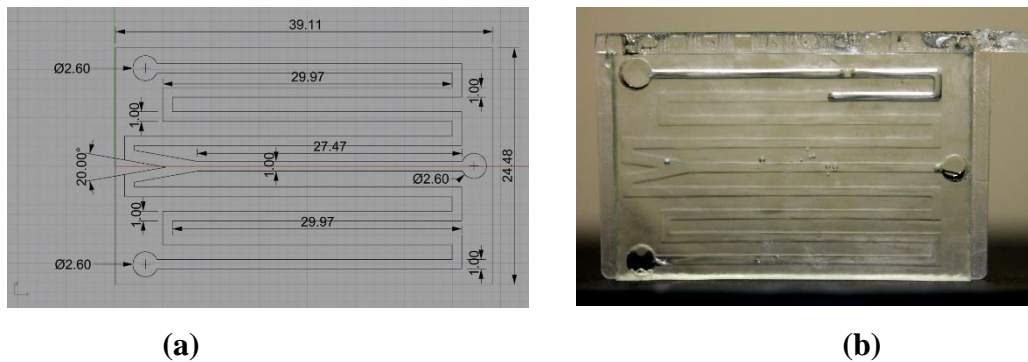


Figure 4.1 (a) Geometry (b) 3D Printed Output of the Optofluidic Microviscometer using Rhinoceros Ver. 5.10

The design was aimed to maintain a laminar flow in the field when the two streams, A and B, are united and thus prevent uncontrolled convective mixing [5]. The interface position for measurement was taken at the midpoint of the length of the main channels i.e. 13.75 mm. Various approach angles, ranging from 5 degrees to 90 degrees, were considered. The higher the angle of approach, the more the instability in flow was found. Hence, after careful deliberations and testing, the best approach angle for each side of the channel for the analysis was found to be in the range of 10-20 degrees.

4.3 SAMPLE PREPARATION AND EXPERIMENTAL SETUP

The samples that were tested using the 3D printed microviscometer were prepared based on the careful study and analysis done by students in the local community of various states in India. The individual milk producers and distributors do not share such critical information as it may lead to a disclosure of their product

selling. Hence, careful tactics were applied wherein close bonding with these producers was developed which led to the identification of various adulterants used in the milk being sold locally. The major adulterants were found to be water, flour (corn and wheat based), starch (corn and potato based), urea and detergents. The use of detergent was just to induce the bubble effect in the increased quantity of milk (after the addition of water) and hence the quantity was found to be very miniscule [93].

In the case of urea, it is used in a very minute quantity for the enhancement of the viscosity in the milk so that water can be added to further increase the quantity. The major adulterants as per the usage statistics are water, flour and starch. The milk sample for the investigation was taken from the local distributor after careful bargaining and tested using the standard Anton Parr rheometer. The average dynamic viscosity of the pure milk at 20⁰C was found to be 19.10 mPa.s. The reference fluid glycerol was procured from Sigma Aldrich India and the average dynamic viscosity was found to be 430.70 mPa.s at 20⁰C. The viscosity of the unadulterated and adulterated milk can also vary depending on the composition, temperature and the age of the milk. But the variation w.r.t to these was not considered for the analysis.

The concentrations of each adulterant in milk was judged and prepared based on direct inputs from these milk producers. In the case of flour, the mixing was carried out in the range of 150 to 200 grams in 5 kilograms of milk which would amount to 3 to 4 wt. % of the overall concentration. Starch was usually added in the range of 100 to 150 grams in 5 kilograms of milk resulting in 2 to 3 wt. % of the adulterant in milk. Since urea was found to be toxic, only a meagre 1 to 2% was added in milk. The samples with adulteration were prepared from 0.5% till 10% for the solid adulterants and water was added to this ratio only in the case of flour. Water was added in the range of 5-95% for testing purposes. Hence, in total

80 samples were prepared and tested using the optofluidic microviscometer and the rheometer.

The experimental setup comprised of the 3D printed optofluidic microviscometer, two peristaltic pumps for inlets, silicone rubber tubing's, pure glycerol as the reference fluid, adulterated milk samples and a Leica Microscope (Model-DFC3000G) for width occupancy measurement and analysis. The entire schematic of the setup was arranged in a fashion as shown in Figure 4.2 (a).

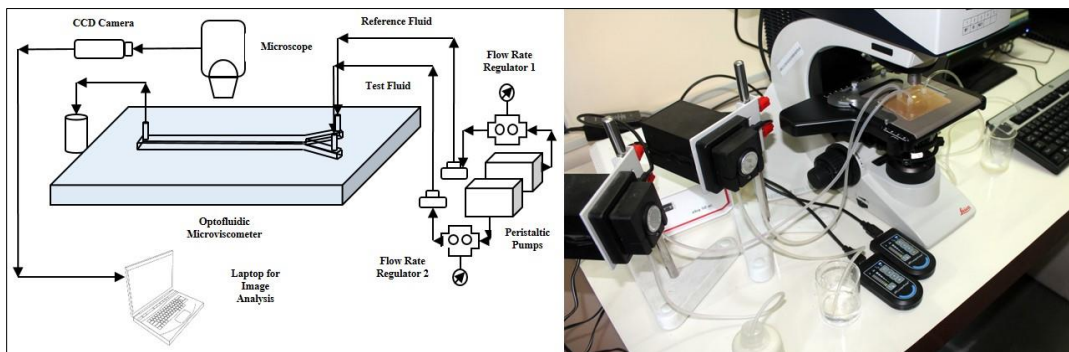


Figure 4.2 (a) Schematic of the Setup (b) Actual Experimental Setup

The reference fluid was taken as pure glycerol and the samples of the adulterated milk were taken as mentioned in the previous sections for the testing and analysis. All the experimental investigations were carried out at standard atmospheric pressure of 1 atm and temperature of 20⁰ Celsius. All the experiments were carried out inside the laboratory considering all the precautionary measures and safety standards. As per the Hagen Poiseuille flow equation, for two immiscible fluids to occupy same width inside the channel, their flow rates at the input should be adjusted accordingly. However, if the flow rates at the input are kept the same, both the fluids will occupy different widths depending on their viscosity.

The two liquids in the OMV were made to flow inside the channel at the same flow rate of 4.5 $\mu\text{L}/\text{min}$. The figure 4.3 shows the measurement of the sample

fluid inside the microchannel using the live recording of the fluorescence microscope for flour adulteration in milk at 2%, 4%, 6% and 8%.

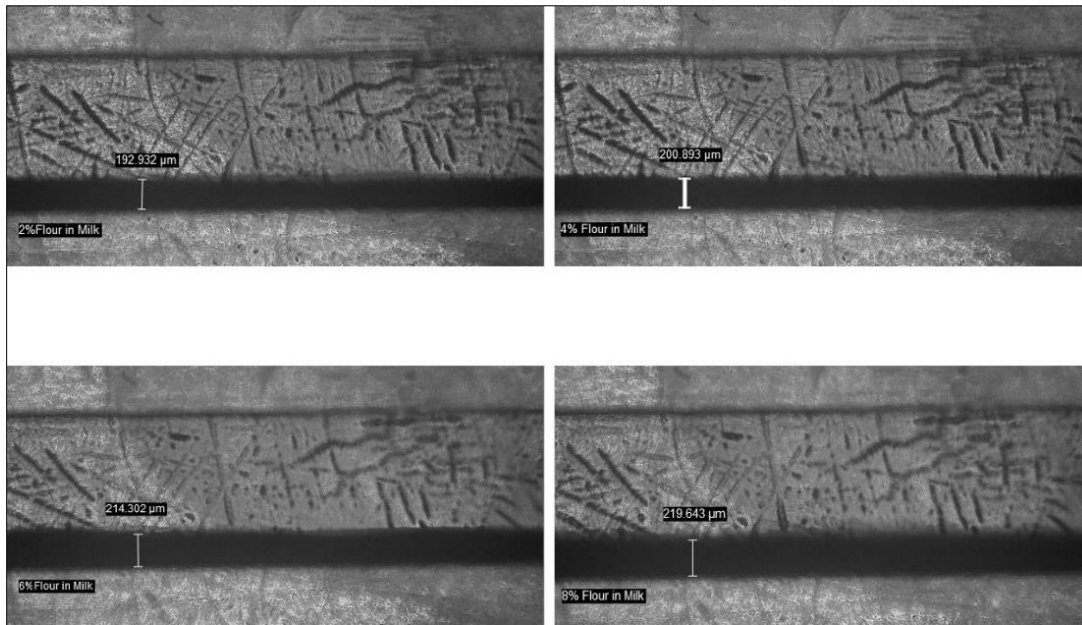


Figure 4.3 Biphasic Interface Position Measurement for Flour in Milk using the OMV

4.4 RESULTS AND DISCUSSION

4.4.1 WATER ADULTERATION IN MILK

The figure 4.4 clearly shows the variation of channel occupancy width with the decrease in the viscosity of the milk due to the gradual increase in the water content. Water is the most commonly available adulterant in milk whereby the adulteration quantity can be to an extent of 70% [94]. Upon careful observation, it is evident that the regression plot is polynomial in nature. The reason could be attributed to the fact that water is miscible in glycerin. Hence during the flow of the two liquids in the common channel, there could have been a possible diffusion of water from the milk with glycerine. Hence this forms the case of a single

solution (despite both being different fluids initially) inside a channel for which the fluid follows a parabolic behavior.

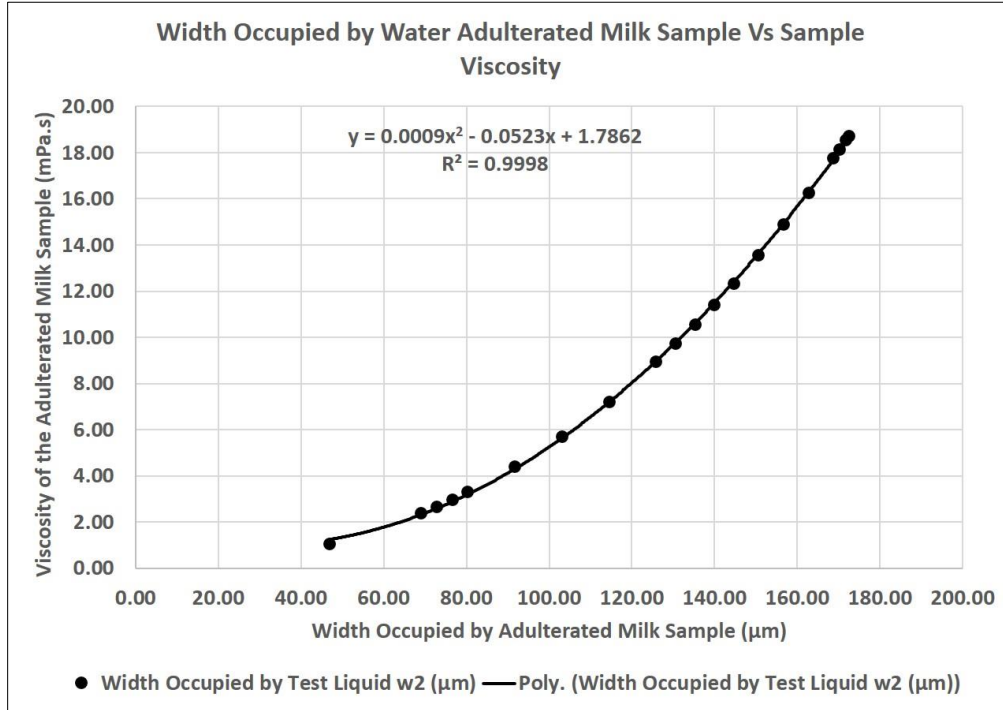


Figure 4.4 Width Occupied by Water Adulterated Milk Sample Vs Sample Viscosity

4.4.2 FLOUR ADULTERATION IN MILK

The most commonly used adulterant in milk is flour [95] as the mixture in combination with hot water remains is also undetectable till a concentration of 3%. The concentrations of flour used in this experiment was based on the inputs from the local dairy farmers. The linear regression graph shown in figure 4.5 (a) shows that the width occupancy of the adulterated milk samples for each percentage of adulteration. It can be clearly seen that as the percentage of flour in milk is increased, the width occupied by the adulterated sample inside the channel is increased. It is a well-known fact that flour is denser than starch and hence the viscosity value increases in larger proportions when compared to the other

adulterants. The linear equation can be used to determine the value of the viscosity if the width occupied by the fluid in the channel is fed in.

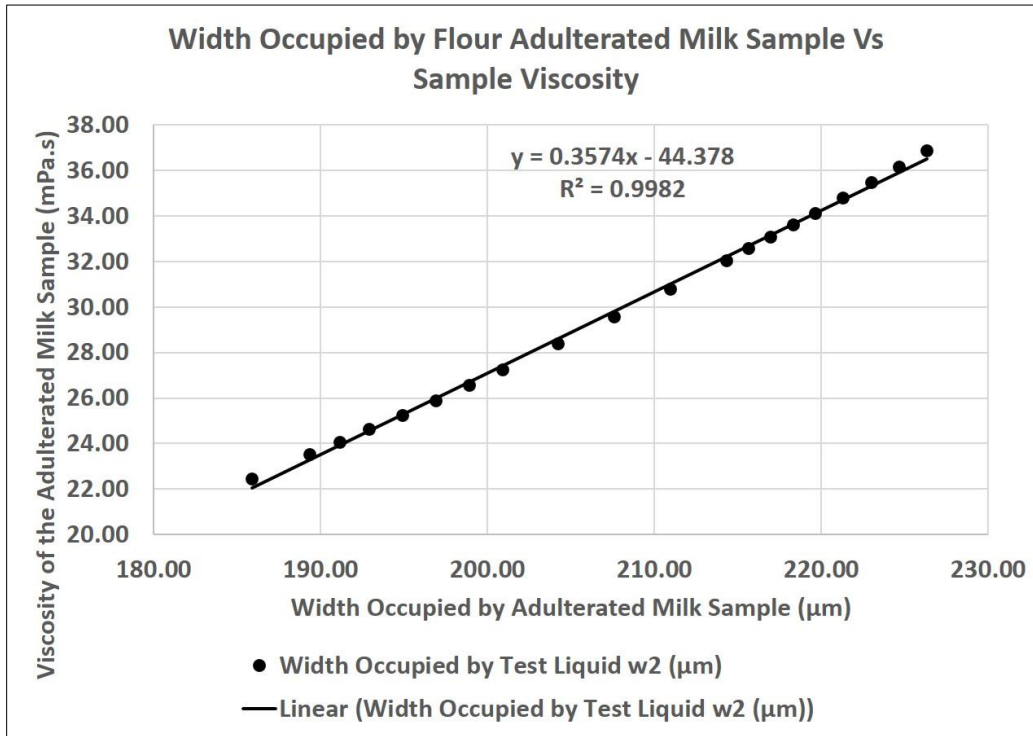


Figure 4.5 (a) Width Occupied by Flour Adulterated Milk Sample Vs Sample Viscosity

In the figure 4.5 (b), the line graph shows the comparison between the values of viscosities measured by the standard rheometer in mPa.s and the values obtained using the microviscometer. The close match between the values of the OMV and rheometer indicates the precision of the device vis-à-vis a standard viscosity measuring laboratory device. There were a few cases wherein the values obtained by the microviscometer was found to be higher than that obtained by the rheometer. This could be due to the instrumental accuracy and precision limitations.

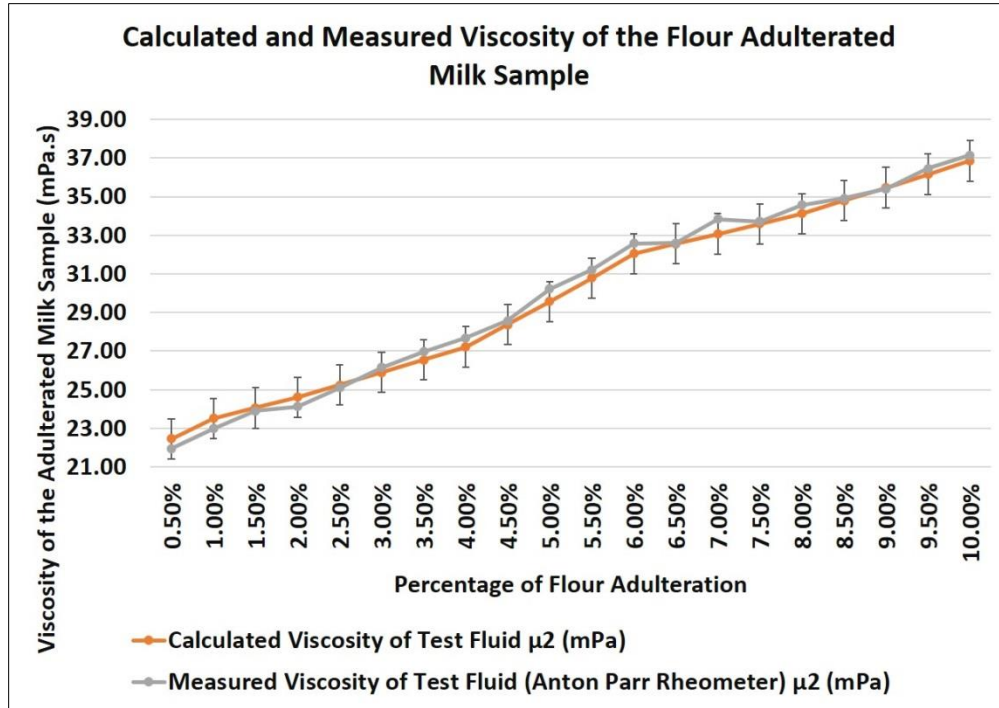


Figure 4.5 (b) Calculated and Measured Viscosity of the Flour Adulterated Milk Sample

4.4.3 STARCH ADULTERATION IN MILK

As shown in figure 4.6 (a), the width occupied by the adulterated milk in the microviscometer slowly increases from 176.04 μm to 223.45 μm for 0.5% adulteration to 10% adulteration respectively, thereby indicating the increase in the viscosity on the addition of starch to milk. A linear regression line was derived for measuring starch adulteration in various percentages.

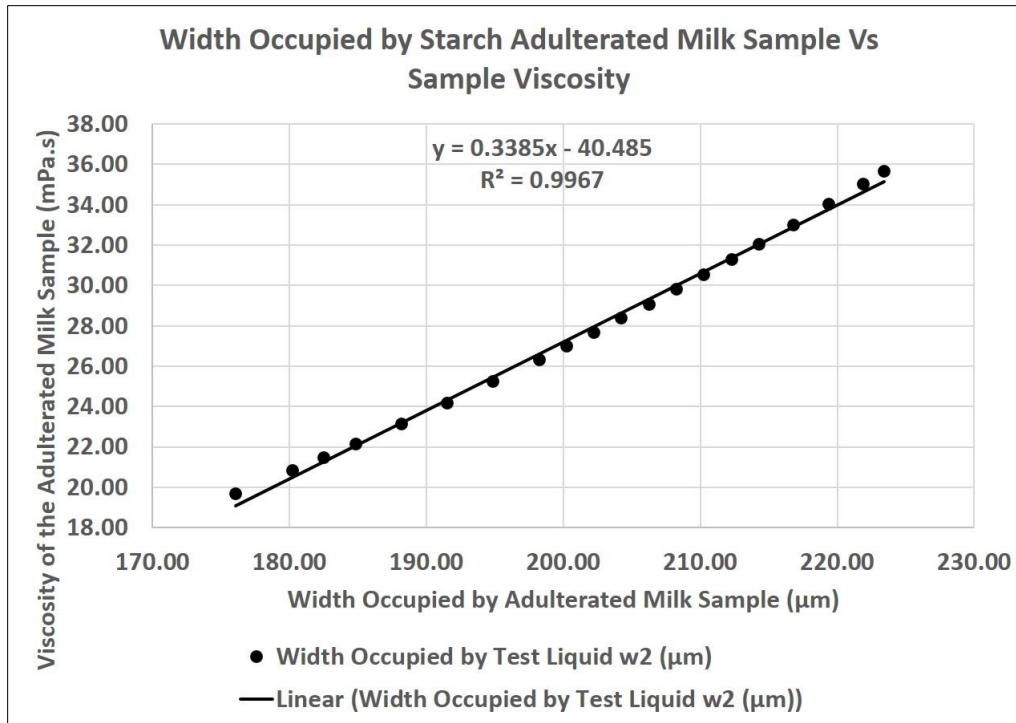


Figure 4.6 (a) Width Occupied by Starch Adulterated Milk Sample Vs Sample Viscosity

There is also a difference in the visual inspection of the milk with flour and with starch. Starch, since it is pure white in color, goes unnoticed to a common man's eyes, whereas the flour particles become vivid if they have not been added to hot water and mixed with milk [96]. Upon addition of starch to milk, an interesting phenomenon was observed. Starch contains a miniscule concentration of glucose. Hence, after the experimentation cycle one can find a lot of residue left over in the channel and proper flushing is to be done for the further use of the device [97]. The figure 4.6 (b) shows a comparison between the calculated and measure values of the adulterated milk samples using the microviscometer and the conventional rheometer. The close adherence between the values specifies the accuracy of the 3D printed microviscometer.

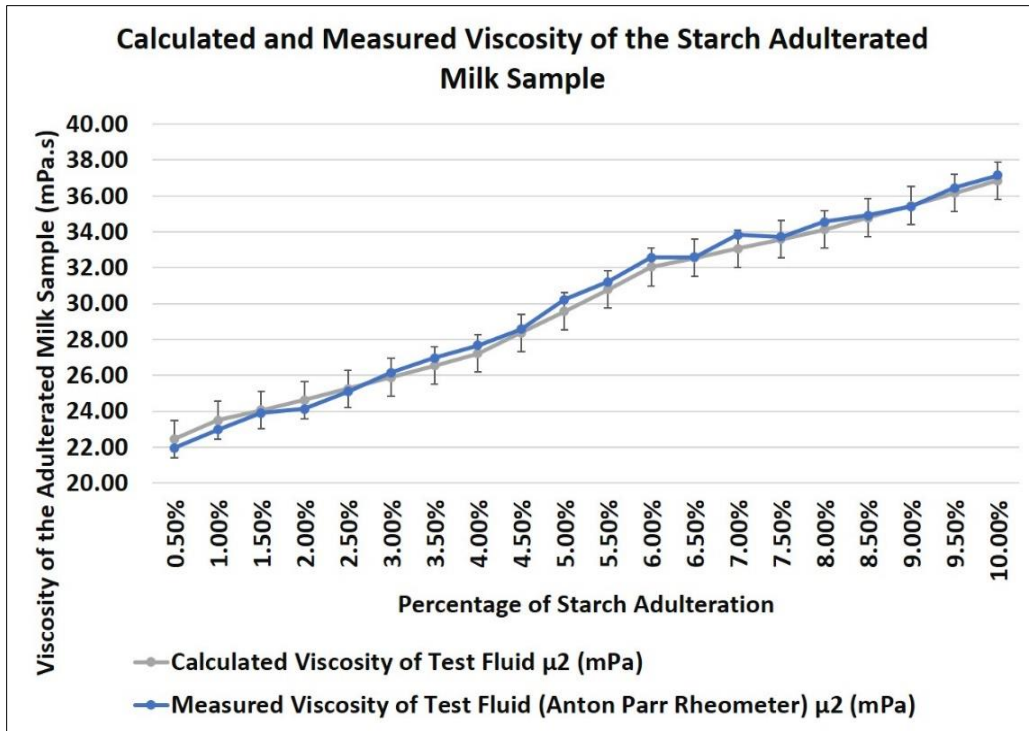


Figure 4.6 (b) Calculated and Measured Viscosity of the Starch Adulterated Milk Sample

4.4.4 UREA ADULTERATION IN MILK

In the case of urea adulteration in milk the figure 4.7(a), shows that when 0.5% of urea is mixed with the milk then the width occupied by the sample in the channel was found to be 175 μm which is lower in comparison to flour (186 μm) and slightly lower in comparison to starch (176 μm). Based on the experimental data, a linear regression line was fit to establish a relationship between the viscosity and the width occupied in the channel, which may be used to measure the extent of urea adulteration in milk.

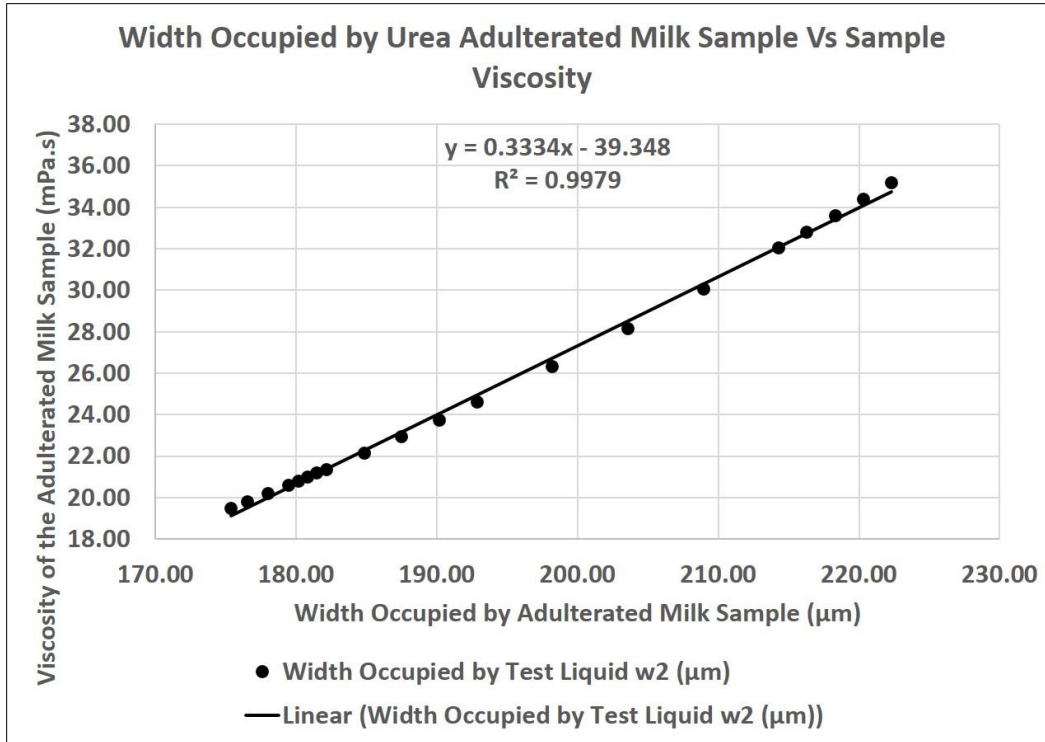


Figure 4.7 (a) Width Occupied by Urea Adulterated Milk Sample Vs Sample Viscosity

As the content of urea in milk was increased from 0.5% to 5% there is sudden increase in occupancy of adulterated milk in Y shape micro channel device. The calculated and measured values of the viscosity for the urea adulterated milk samples in shown in figure 4.7 (b). There are many sensors which have been devised by fellow researchers namely enzyme thermistor, potentiometric biosensor, electronic tongue etc. Most of them have the limitation of lab based experimentation and requirement of an experience operator which has been reduced in the optofluidic microviscometer [98-100].

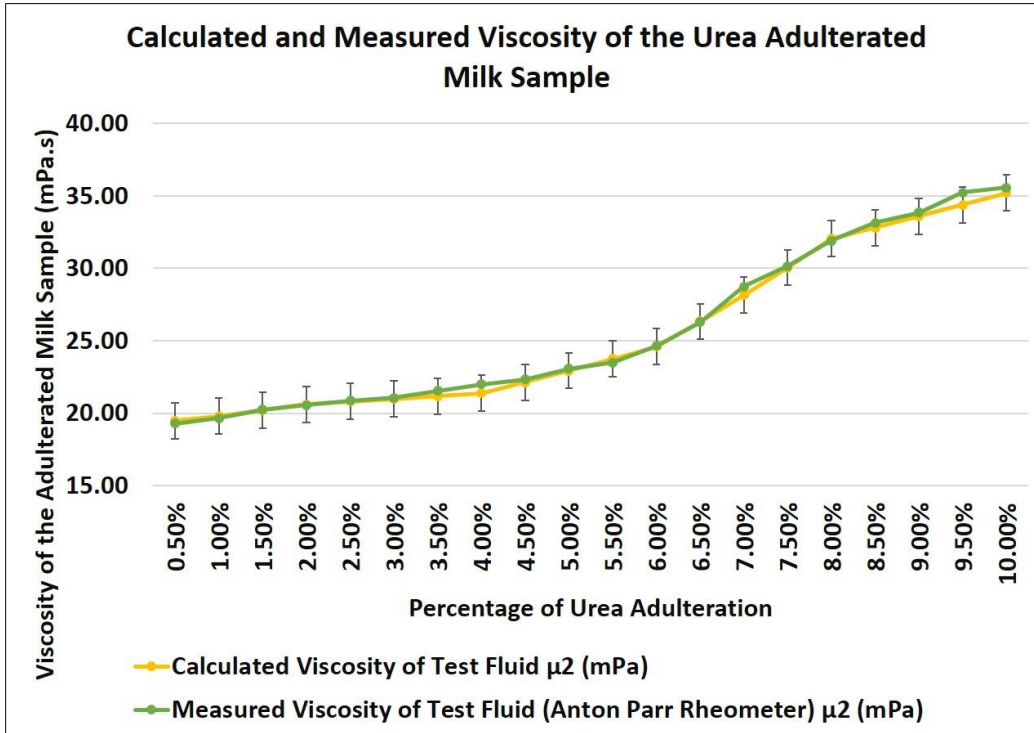


Figure 4.7 (b) Calculated and Measured Viscosity of the Urea Adulterated Milk Sample

The experimental output clearly indicates that the real-time detection and monitoring of milk adulteration can be done using this device. According to the width value occupied by the individual fluids flowing in the device, the dynamic viscosity of the unknown sample can be calculated using the derived theoretical model for the flow of two immiscible fluids in a micro-channel. The analysis also proves that the addition of an adulterant in milk invariably affects its viscosity thereby making it easy to detect. This device is accurate to measure even 1% of adulteration in milk thereby making it one of the most reliable and robust measurement device. This fully automated and robust device can be fabricated using the well-established 3D printing technique. It also has a high durability and is re-usable after flushing the reference fluid.

CHAPTER V

5. 3D PRINTED OPTICAL MICROVISCOMETER FOR THE TESTING OF AUTOMOBILE FUEL ADULTERATION

5.1 OVERVIEW

Fluids, the term clearly indicates the expansive span of all the liquids present in the table of possibilities of a state of matter wherein the flow is in between that of a gas and a solid [101]. Fluids form an important aspect in fields ranging from industrial applications to day-to-day activities. Industrial fluids range from lubricants, fuel, engine oils, biofuels, machinery oils and drilling fluids. In day-t-day household activities the major fluids used include water, milk, honey, brewed liquids, etc. [102-104]. All these liquids undergo or do a particular action with respect to their purpose of usage. In order to determine the particularity of a fluid, it has to undergo various tests and measurements. Most of these tests depend on their physical and chemical properties [105]. These tests are either carried out in big characterization facilities or using macro-scale devices designed for their purpose with proper governmental authorization and seals [105, 106].

It is well known that the additives added to any liquid fuel directly affects the performance and efficiency of any automobile. The various physical properties that govern the fluids include viscosity, concentration, additives, adulterants, boiling point, melting point, etc. Hence, developing a sensor, based on the physical properties of such fluids, can provide a reliable and effective solution to detect and monitor adulterations in such fluids. Amongst various available devices employed to test different physical properties of fluids, the key issues which decide the widespread applicability of the device are dimension, precision and price of the device. Although there are many devices which are used for testing and monitoring applications, they require multifaceted measurement,

expensive equipment, allowance of more time and a familiar machinist [107, 108].

This chapter covers the experimental validation of the optofluidic microviscometer which performs fuel adulteration measurement by analyzing the dynamic viscosity as one of the physical properties and its variations. The working principle in this case is viscosity dependent width capture by two immiscible fluids flowing in a rectangular microchannel under the same flow rate. The tests were conducted for several blending ratios between petrol, diesel and kerosene.

5.2 SAMPLE PREPARATION AND EXPERIMENTAL SETUP

The petrol, diesel and kerosene samples were procured from a petrol station in Dehradun, India. The blending of three liquids was done at different ratios to understand the change in the interface position based on change in the dynamic viscosity of the samples. All the pure samples were tested for their dynamic viscosities using a standard Anton Parr rheometer. The average dynamic viscosity of the pure petrol at 25⁰C was found to be 0.81 mPa.s. The average dynamic viscosities of pure diesel and pure kerosene at 25⁰C was found to be 2.64 mPa.s and 2.10 mPa.s respectively. Pure glycerol could not be used directly as the dynamic viscosity of it was so high that it did not allow the flow of the second fluid inside the channel. Therefore a 20wt% glycerol solution was used which had a dynamic viscosity of 1.125 mPa.s. The viscosity of the fuel samples also vary depending on composition and temperature. But the variation w.r.t to these was kept to be minimum and the experiment was done under set temperature conditions. The samples were prepared in four categories. The first included the adulteration of petrol with diesel. The second was kerosene in petrol followed by kerosene in diesel. All the above three categories were done in the range of 100:0 to 0:100 with increments in 20%. The last category saw the mixture of all the

three fuel samples in an ad-hoc manner with 20% increment in each fuel added to the sample.

#	Sample Name	Content 1	%	Content 2	%	Content 3	%
P+D							
1	100P-0D	Petrol	100%	Diesel	0%	-	-
2	80P-20D	Petrol	80%	Diesel	20%	-	-
3	60P-40D	Petrol	60%	Diesel	40%	-	-
4	40P-60D	Petrol	40%	Diesel	60%	-	-
5	20P-80D	Petrol	20%	Diesel	80%	-	-
6	0P-100D	Petrol	0%	Diesel	100%	-	-
P+K							
7	100P-0K	Petrol	100%	Kerosene	0%	-	-
8	80P-20K	Petrol	80%	Kerosene	20%	-	-
9	60P-40K	Petrol	60%	Kerosene	40%	-	-
10	40P-60K	Petrol	40%	Kerosene	60%	-	-
11	20P-80K	Petrol	20%	Kerosene	80%	-	-
12	0P-100K	Petrol	0%	Kerosene	100%	-	-
D+K							
13	100D-0K	Diesel	100%	Kerosene	0%	-	-
14	80D-20K	Diesel	80%	Kerosene	20%	-	-
15	60D-40K	Diesel	60%	Kerosene	40%	-	-
16	40D-60K	Diesel	40%	Kerosene	60%	-	-
17	20D-80K	Diesel	20%	Kerosene	80%	-	-
18	0D-100K	Diesel	0%	Kerosene	100%	-	-
P+D+K							
19	0P-0D-100K	Petrol	0%	Diesel	0%	Kerosene	100%
20	0P-20D-80K	Petrol	0%	Diesel	20%	Kerosene	80%
21	0P-40D-60K	Petrol	0%	Diesel	40%	Kerosene	60%

22	0P-60D-40K	Petrol	0%	Diesel	60%	Kerosene	40%
23	0P-80D-20K	Petrol	0%	Diesel	80%	Kerosene	20%
24	0P-100D-0K	Petrol	0%	Diesel	100%	Kerosene	0%
25	20P-0D-80K	Petrol	20%	Diesel	0%	Kerosene	80%
26	20P-20D-60K	Petrol	20%	Diesel	20%	Kerosene	60%
27	20P-40D-40K	Petrol	20%	Diesel	40%	Kerosene	40%
28	20P-60D-20K	Petrol	20%	Diesel	60%	Kerosene	20%
29	20P-80D-0K	Petrol	20%	Diesel	80%	Kerosene	0%
30	40P-0D-60K	Petrol	40%	Diesel	0%	Kerosene	60%
31	40P-20D-40K	Petrol	40%	Diesel	20%	Kerosene	40%
32	40P-40D-20K	Petrol	40%	Diesel	40%	Kerosene	20%
33	40P-60D-0K	Petrol	40%	Diesel	60%	Kerosene	0%
34	60P-0D-40K	Petrol	60%	Diesel	0%	Kerosene	40%
35	60P-20D-20K	Petrol	60%	Diesel	20%	Kerosene	20%
36	60P-40D-0K	Petrol	60%	Diesel	40%	Kerosene	0%
37	80P-0DN-20K	Petrol	80%	Diesel	0%	Kerosene	20%
38	80P-20D-0K	Petrol	80%	Diesel	10%	Kerosene	10%
39	100P-0D-0K	Petrol	100%	Diesel	0%	Kerosene	0%

Table 5.1 Sample List of Conventional Fuels

A total of 39 samples as shown in the Table 5.1 were prepared and tested using the optofluidic microviscometer and verified with the measurement results of the Anton Parr rheometer for accuracy and precision. The experimental setup consisted of two peristaltic pumps, silicone tubing's, optofluidic microviscometer and a Leica microscope with a high speed camera for quick capture and width measurement. All the experimental investigations were carried out at 25⁰ Celsius and at an atmospheric pressure of 1 atm. The controlled environment was possible inside a laboratory considering all safety and precautionary standards.

5.3 RESULTS AND DISCUSSION

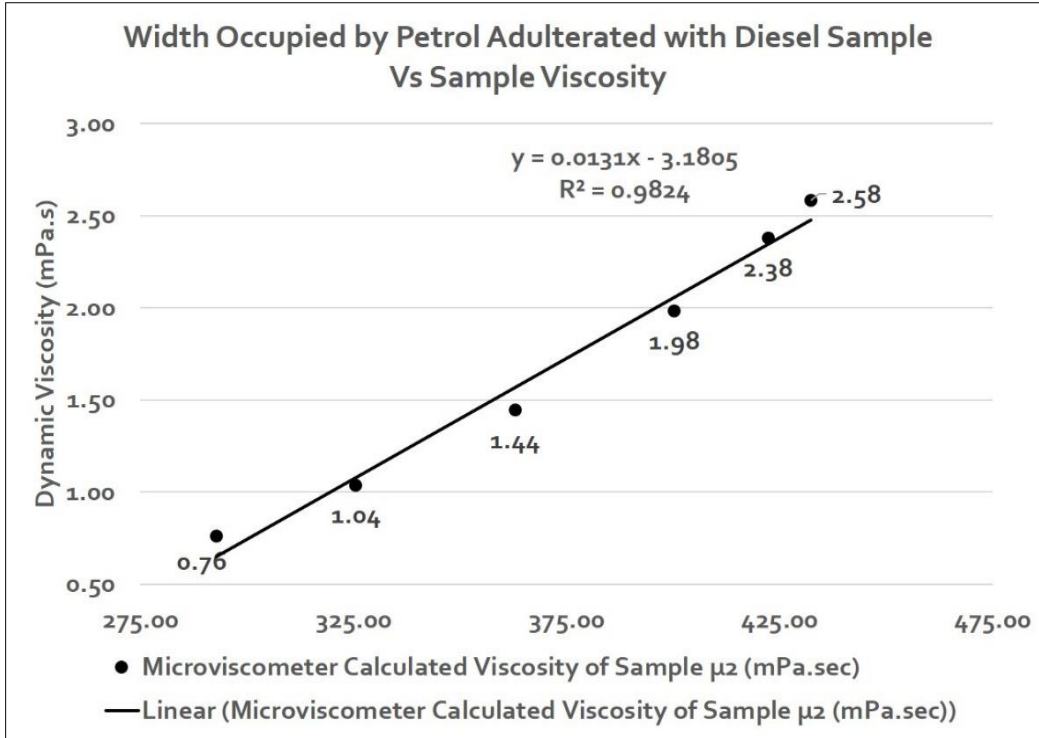


Figure 5.1 (a) Width Occupied by Petrol Adulterated with Diesel Sample Vs Sample Viscosity

As shown in figure 5.1 (a), the addition of diesel to petrol clearly shows that the interface shift is towards the higher side. This is because diesel has a density of 0.83 gm/cm^3 at 25^0C and petrol has a density of 0.74 gm/cm^3 at 25^0C . Hence, on the increase in concentration of diesel in petrol, the viscosity of the adulterated sample keeps on increasing. This may be attributed to the width occupancy of the adulterated sample in the channel with 20wt% glycerol solution as the reference fluid. Hence upon addition of diesel to petrol the viscosity increases which results in increase of the width occupied by the mixture. The figure 5.1 (b) shows the measured and calculated viscosities of various samples. It can be clearly seen that the values obtained using the microviscometer are pretty much close to the ones measured by the rheometer.

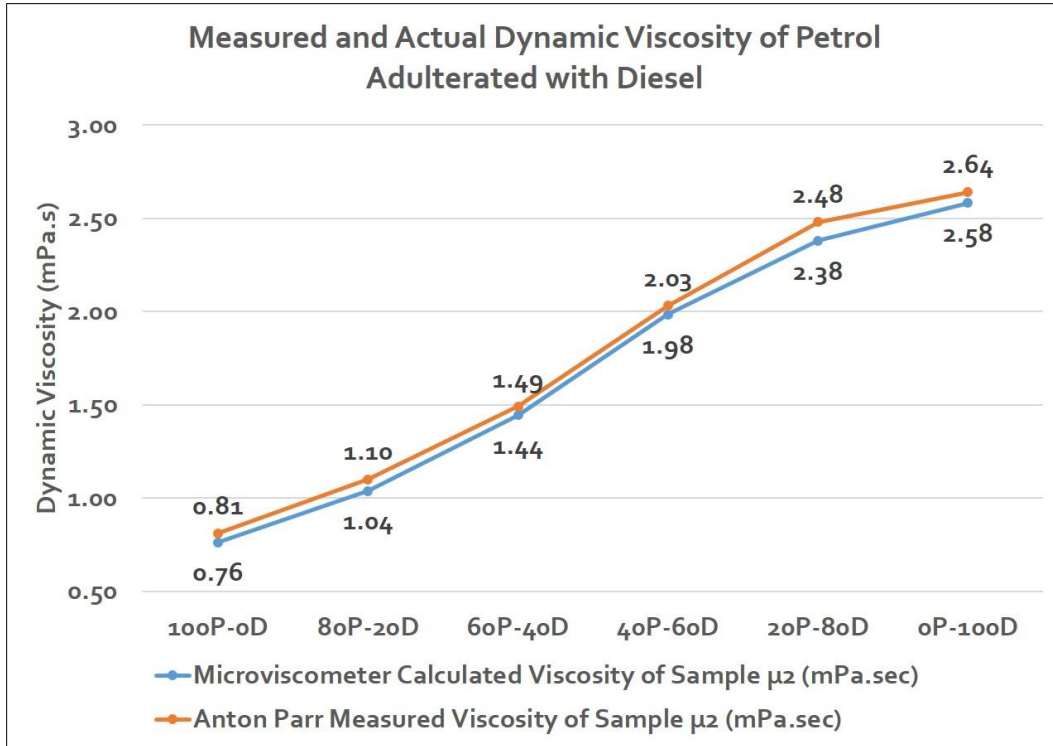


Figure 5.1 (b) Measured and Actual Dynamic Viscosity of Petrol Adulterated with Diesel

In the second case of petrol adulteration with kerosene shown in the figure 5.2 (a), it can be seen that the variation of viscosity is there but not as significant as in the case of diesel in petrol. This can be attributed to the fact that the density of kerosene is in between that of the petrol and diesel i.e. 0.78 gm/cm^3 at 25°C . Hence the interface shift is in such a way that the dynamic viscosity gets increased from a value of $0.93 \text{ mPa}\cdot\text{sec}$ for 20% addition of kerosene to $1.75 \text{ mPa}\cdot\text{sec}$ at 80% addition of kerosene to petrol.

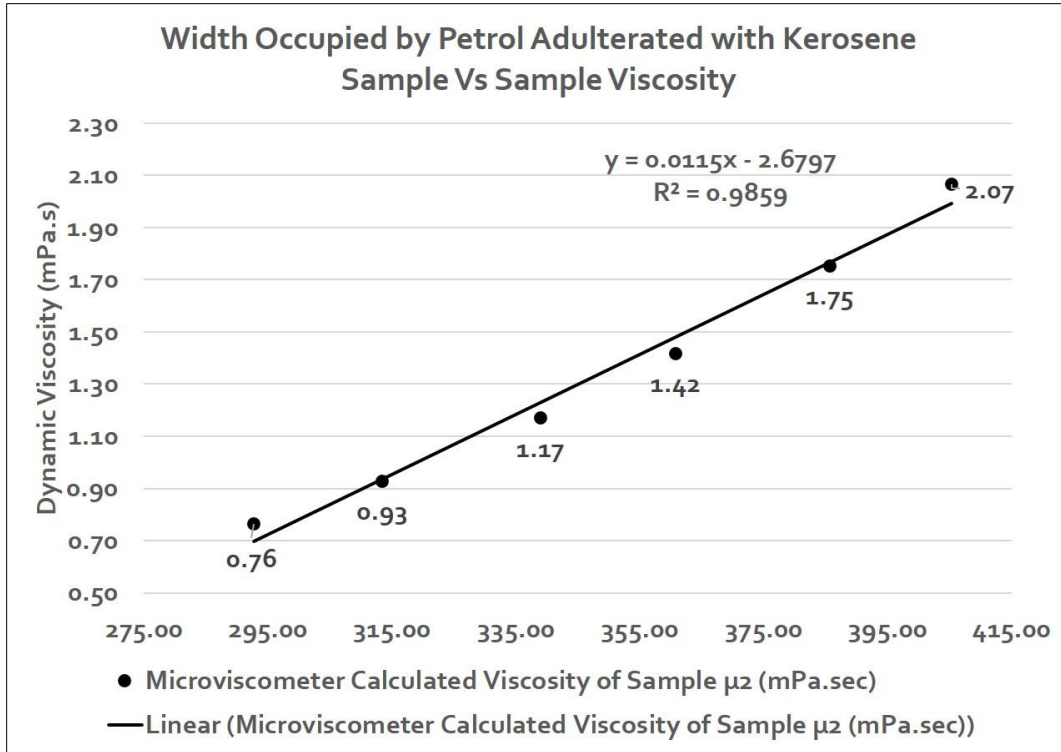


Figure 5.2 (a) Width Occupied by Petrol Adulterated with Kerosene Sample Vs Sample Viscosity

The figure 5.2 (b) shows the values of the dynamic viscosity obtained from the rheometer and the microviscometer as a comparison. In the case of the 60P-40K, the values almost match showing the accuracy of the 3D printed microviscometer. The other values also vary within a close proximity of $\pm 5\%$. Hence, it is evident that the microviscometer can be slightly tuned in order to get a more exact value of the viscosity.

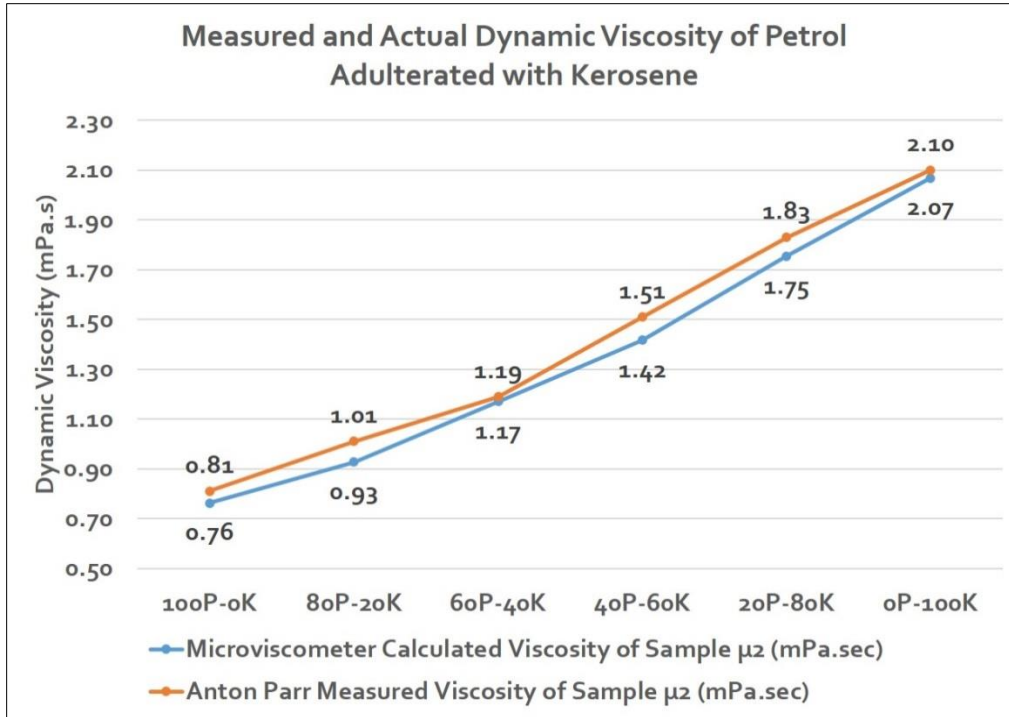


Figure 5.2 (b) Measured and Actual Dynamic Viscosity of Petrol Adulterated with Kerosene

Considering the case of kerosene in diesel, it is clearly evident that these two are the densest of the three sample lot. Hence the addition of kerosene would actually decrease the sample's viscosity as can be seen in the figure 5.3 (a) and (b). The linear regression line fit clearly indicates the linear relationship between the width occupied by the adulterated sample and its viscosity. The decrease in the width occupied upon addition of kerosene can be used to obtain the value of the viscosity using the theoretical derived equation.

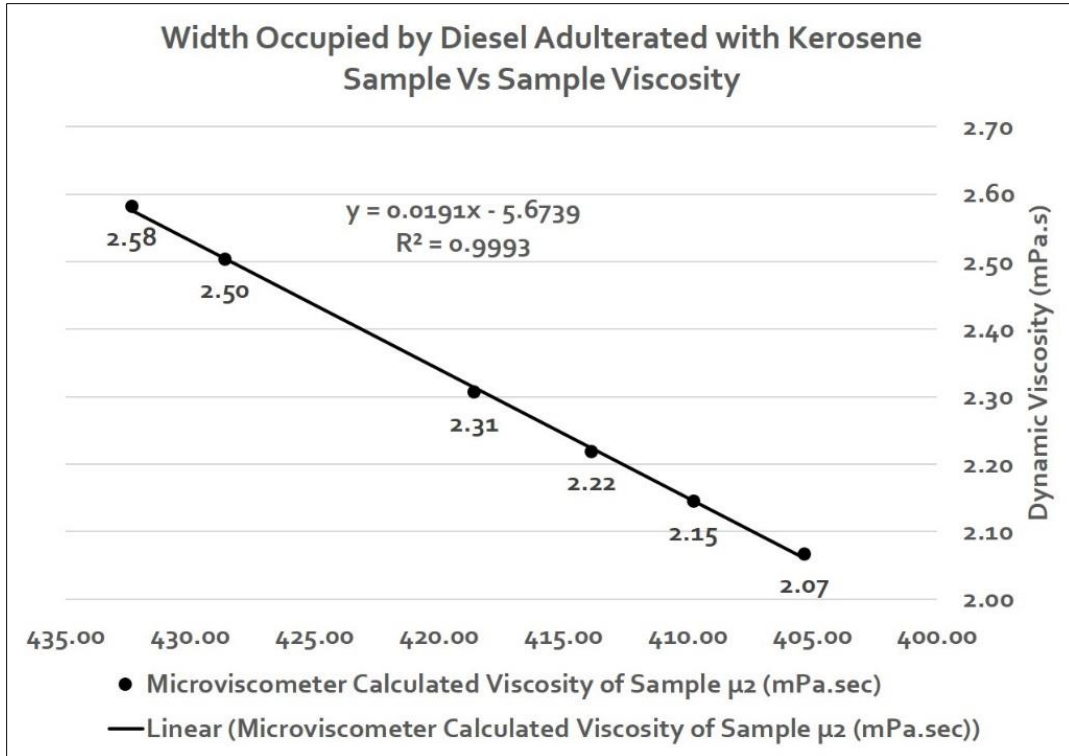


Figure 5.3 (a) Width Occupied by Diesel Adulterated with Kerosene Sample Vs Sample Viscosity

The figure 5.3 (b) shows the comparison between the dynamic viscosity values obtained by the microviscometer and the conventional rheometer. The value for the viscosity obtained by the microviscometer starts at 2.58 mPa.sec for pure diesel and upon gradual addition of kerosene to the sample, the viscosity value reduces to a mark wherein finally it reaches close to that of pure kerosene 2.07 mPa.sec. This marked change in the viscosity of the sample is also close to the values obtained using the conventional Anton Parr rheometer which measured the viscosity values for all the samples.

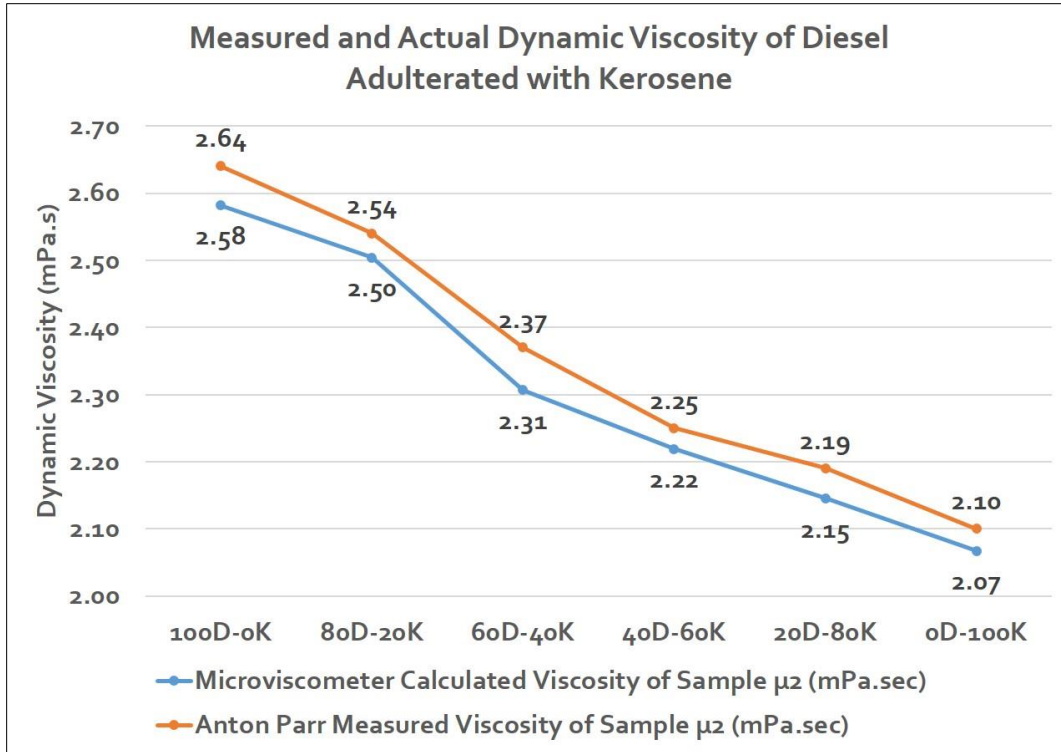


Figure 5.3 (b) Measured and Actual Dynamic Viscosity of Diesel Adulterated with Kerosene

The last scenario was the adulteration of petrol with both diesel and kerosene. The three fluids were mixed considering one of the fluid concentrations to be fixed. The petrol concentration was fixed for every value between 0 to 100% (0, 20, 40, etc.) and the diesel and kerosene were added progressively. The linear regression plot shown in the figure 5.4 (a) indicates that the addition of the two adulterants in petrol also follows a linear pattern upon addition of kerosene and diesel to petrol samples. The mixture was immiscible with glycerine. Hence the theoretical derivation of the two immiscible fluids flowing inside a rectangular channel was verified for the measurement of viscosity based on width capture of the adulterated fuel samples.

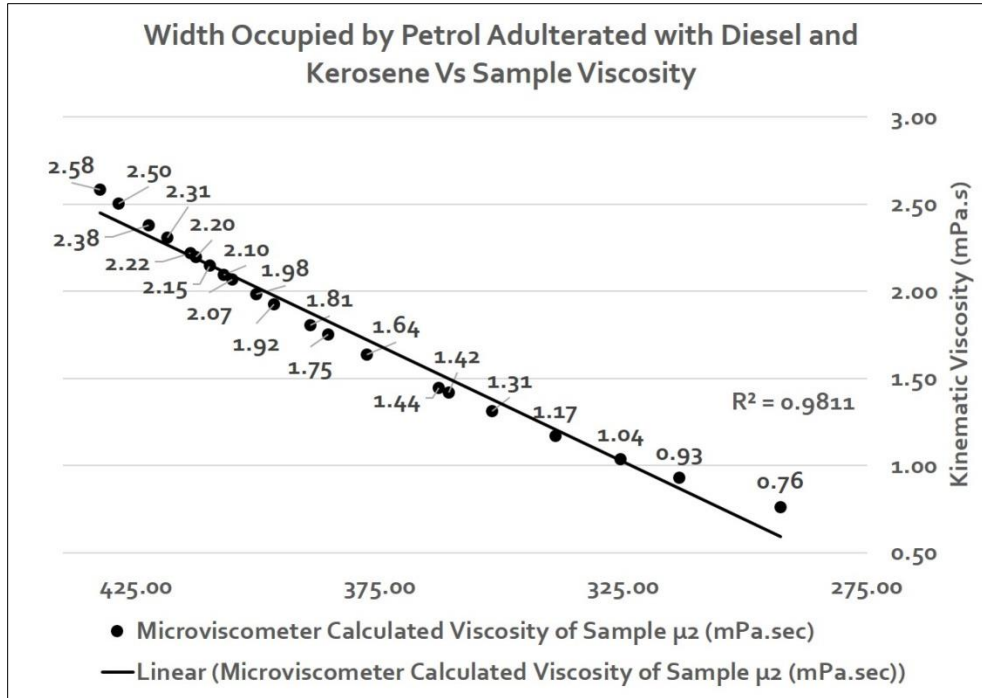


Figure 5.4 (a) Width Occupied by Petrol Adulterated with Diesel and Kerosene Vs Sample Viscosity

The graph shown in the figure 5.4 (b) indicates the variations in the dynamic viscosity when all the three fuel samples are mixed in pre-defined proportions. The portion 'A' in the graph indicates the addition of diesel and kerosene to 0 wt% of petrol. Hence this follows the exact same pattern of kerosene in diesel shown in the figure 5.3 (b). The last sample in this set comprises of pure diesel having a dynamic viscosity of 2.58 mPa.sec. The portion marked as 'B' in the graph shows the variation in the viscosity of 20 wt% of petrol when diesel and kerosene are added in the remaining 80 wt% in proportions of 20 wt% each. The first sample contains 20% petrol and 80% kerosene thereby showing values in similarity to that shown in figure 5.2 (b). The last sample is a combination of 20 wt% of petrol and 80 wt% of diesel following the values obtained parallel to the ones in figure 5.1 (b). The 'C' portion in the graph shows the samples wherein petrol is fixed at 40 wt% and the remaining portion is shared by kerosene and diesel. The 60 wt% petrol sample (Section 'D') with the remaining shared

between kerosene and diesel contains just three samples in a progressive list. The overall viscosity graph reaches the last peak in the ‘E’ section wherein just two samples can be formed with petrol occupying 80 wt% in the sample mixture.

The first and the last sample in the final mixture is pure kerosene and pure petrol showing values of 2.10 mPa.sec and 0.76 mPa.sec as their dynamic viscosities. Upon increase in concentration of kerosene in the sample the viscosity does increase but to the extent as in the case of adding diesel to the sample. The addition of diesel fuel to the other components caused the maximum variation in the viscosity as can be seen in the first peak. The second peak that shows the viscosity of the mixture of petrol and diesel in a 1:4 ratio is comparatively lesser than the first peak. The third peak shows that the viscosity of the mixture of petrol and diesel in a 2:3 ratio being lower than the former followed by the fourth and final peak showing the mixture in a 3:2 ratio.

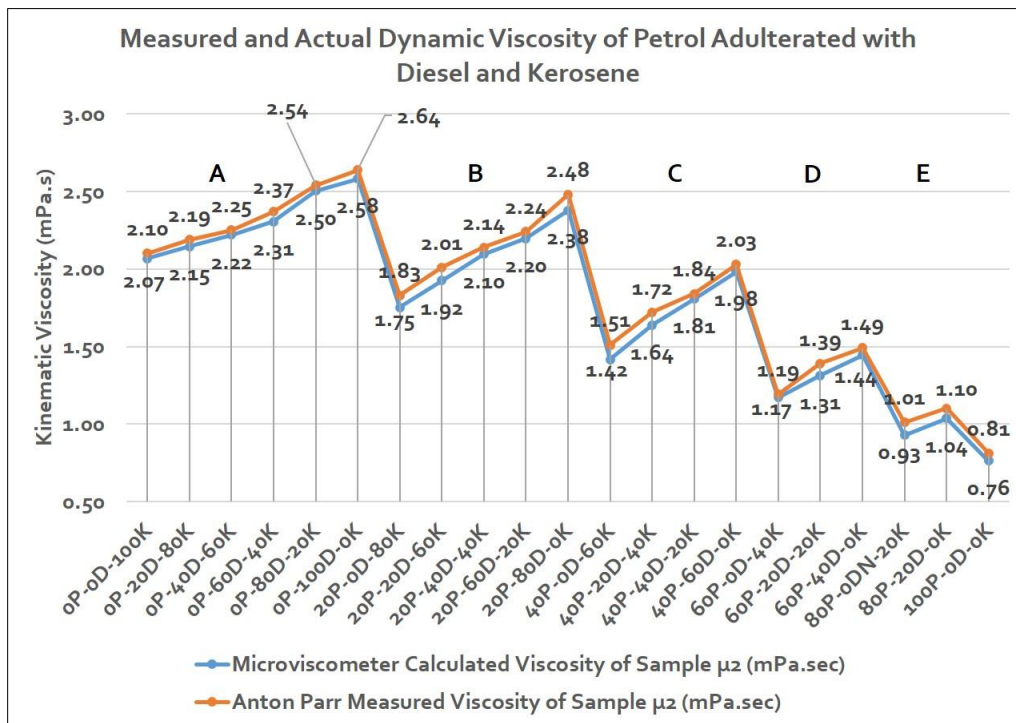


Figure 5.4 (b) Measured and Actual Dynamic Viscosity of Petrol Adulterated with Diesel and Kerosene

Upon observation, it becomes evident that the value of viscosity follows a linear pattern in the reverse order. This indicates that the sample containing more of petrol shows a shift towards the higher viscosity values when kerosene or diesel concentration in the sample increases. The comparison of the portions A and B in the figure 5.4 (b) with figures 5.3 (b) and 5.2 (b) respectively shows adherence to the viscosity values with two sample mixtures thereby validating the results. The line graphs in figure 5.4 (b) also show a close correspondence between the values of dynamic viscosities obtained using the optofluidic microviscometer and the standard rheometer. This study thereby provided a novel method of calculating viscosity of fuel samples on a simple microfluidic device for detecting automobile fuel adulteration. The values obtained indicate the accuracy and precision of the device in measuring adulteration. This device can further be put to test the possibility of its usage in other applications.

CHAPTER VI

6. CONCLUSION AND FUTURES COPE

This thesis reports a method to calculate the viscosity of test samples using a simple y-shaped microfluidic device. Both the test fluid and the reference fluid are made to flow in a rectangular micro-channel under the influence of a fixed flow rate. The concentration dependent viscosity of the sample can be found out based on the increase or decrease of width occupancy inside the microfluidic channel. The viscosity of the fluid is then estimated using the modified Hagen Poiseuille's law which needs the width occupied by the fluids flowing in the channel as an input. This method has been shown to do real-time detection and monitoring of adulteration in several fluids like milk, diesel, petrol, etc.

The experimental analysis was performed for three different applications. The test samples were run in the optofluidic microviscometer and a more conventional Anton Parr rheometer to determine the accuracy and precision of the 3D printed device. A method was devised to determine the biodiesel blend based on the percentage of micro-channel occupancy by each of the biodiesel blends ranging from B20 to B100. The device was then used to test the variation in the viscosity of milk upon the addition of four typically used adulterants namely water, flour, starch and urea. Ratios ranging from 5% to 95% was tested in the case of water. Ratios ranging from 0.5% to 10% was tested for the solid adulterants. The percentage of adulteration was derived based on the inputs from local milk producers in the city of Dehradun. The linear equations obtained during the testing could be used to determine the ratio of adulteration in milk based on the width occupancy in the channel. Further, the device was also used to test the dynamic variation of the viscosity in fuels. Petrol, diesel and kerosene was tested in varying combinations namely diesel in petrol, kerosene in petrol, kerosene in

diesel and a mixture of all the three. There were minute but marked variations in the viscosity of the fuel samples upon addition of an adulterant. The device was effective in determining the viscosity of all the test samples in close correspondence to the results obtained using a standard rheometer. Regression analysis was performed to the data obtained from all the three types of experiments. In case of miscible fluids, regression analysis showed parabolic behavior, whereas in case of immiscible fluids, the behavior was found to be linear as derived in the theoretical model.

This lab-on-a-chip (LOC) device was initially fabricated using the conventional micromachining technique wherein limitations like tool size, leakage, need of an experienced operator and complicated designing was encountered. With the advent of the rapid prototyping techniques, the fabrication of the device became cost-effective and simple. The microviscometer was then fabricated by the stereolithography based 3D printing technique using an UV curable acrylic polymer. Once the device design was ready, the entire process of fabrication took less than ten minutes. The 3D printing method of fabrication gave a device which was durable, strong with accurate dimensions and leakage free operation. The embedded microchannels removed the necessity of an extra sheet of acrylic as in the case of micromachining. The device was found to be re-usable, could be re-calibrated and further made into a plug-n-play scheme for its use in different applications.

3D printed microfluidics could be the next step towards flawless bio-medical devices with numerous application ranging from blood coagulation, blood sampling to PT-INR measurement. In the future scope, an electronic version of the microviscometer will be explored which will work on the similar principle i.e. for any fluid, time required to travel a unit distance in a micro-channel, of a given cross-section, is inversely proportional to its viscosity. There will be no reference fluid required for such a device and its electrical output can have higher

possibilities of integration with other integrated control systems. This electronic version of the microviscometer can also be modified for other applications like food adulteration and hemoglobin detection in blood.

The device design for such a prototype would have a straight channel with a side-channel for flushing (to be closed during operation) as shown in figure 6.1 (a). In the main channel, electrodes could be placed along the y-axis at pre-determined locations with known distances of separation. A counter electrode along the main channel will generate a signal upon fluid flow. This will be due to the flow of fluid between the counter electrode and the various y-axis electrodes. A micro-controller and data acquisition system could be incorporated to record the signal generated by the passing of fluid at various positions of the y-axis electrodes in real-time mode. A 3D printed design of the electronic version has been done as shown in figure 6.1 (b) and the electronic circuitry will be the subsequent step forward.

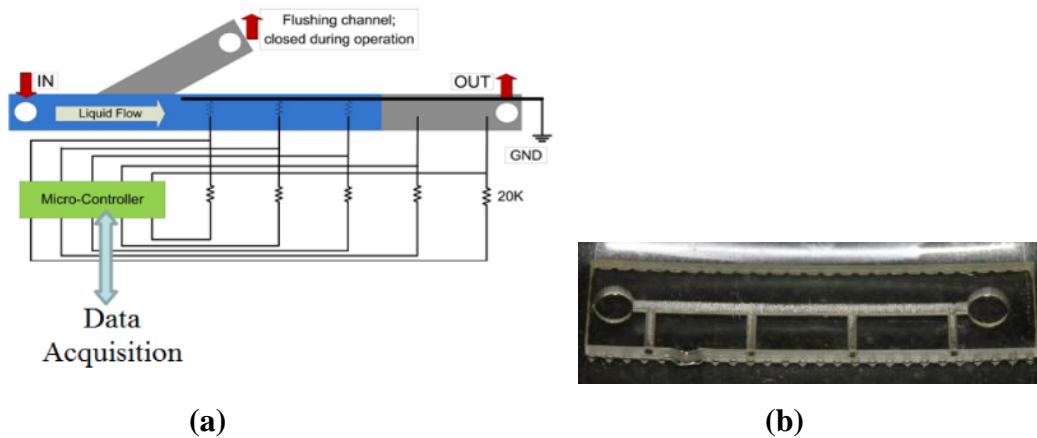


Figure 6.1 (a) Electronic Microviscometer Concept (b) 3D Printed Device

Therefore, the viscosity of the fluid flowing in the main channel can be determined by the Hagen-Poiseuille flow equation, considering 'L' as length between two y-axis electrodes.

$$\mu = \frac{w^2 \Delta P}{2v_m L} = \frac{w^2 \Delta P \Delta t}{2L^2} \quad (26)$$

As we know 'w' (width of the channel in mm), ' ΔP ' (difference in pressure between the inlet and outlet channels in Pascals), and ' Δt ' (time difference to cover the distance 'L'), we can measure the viscosity.

7. APPENDIX A

Flow of a Fluid in a Horizontal Channel

Viscosity has the dominant role in mass transport inside micro-fluidic devices. It is the ratio of shear stress to the velocity gradient in the direction perpendicular to the plane of shear. Being the central property in a micro-fluidic environment, viscosity and its variation may be directly observed and analyzed using LOC devices.

Consider a horizontal micro-channel formed by two parallel plates (made of any typical material, like glass or polymer) as shown in figure 1.1. In order to pass a liquid through the channel a pressure difference between the inlet and outlet is required. The resulting flow of the liquid in the channel is governed by the simultaneous action of the force due to pressure difference and viscous force.

The total force acting on the liquid inside the micro-channel per unit volume may be represented as

$$F_T = F_{\text{Pressure}} + F_{\text{Viscous}} \quad (27)$$

Under the action of this force, the liquid moves with an acceleration of $\frac{dv}{dt}$

$$F_T = \rho \frac{dv}{dt} \quad (28)$$

where ρ is the density of liquid flowing in the channel; v is the velocity of the liquid.

$$\rho \frac{dv}{dt} = F_{\text{Pressure}} + F_{\text{Viscous}} \quad (29)$$

The force due to Pressure (F_{Pressure}) may be calculated by considering a volume element inside the channel with elemental volume as $\Delta x \Delta y \Delta z$, and assuming the pressure gradient mainly along the length of the channel (which is along x -axis) (see figure 7.1) The assumption that pressure gradient is mainly along x -axis (and

is negligible along y and z axes) is valid because the micro-channel has very small dimension (thickness) along the directions perpendicular to x .

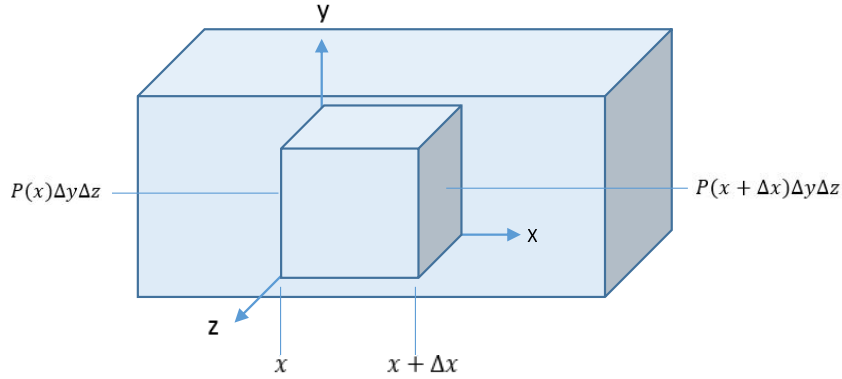


Figure 7.1 Volume Element inside a Micro-channel

The force due to pressure per unit volume on the yz surface of the element may be written as

$$F_{\text{Pressure}} = \frac{(P(x + \Delta x, y, z) - P(x, y, z))dA}{dV}$$

where dA is the area of the yz surface.

$$F_{\text{Pressure}} = \frac{(P(x + \Delta x, y, z) - P(x, y, z))\Delta y\Delta z}{\Delta x\Delta y\Delta z}$$

$$F_{\text{Pressure}} = \frac{(P(x + \Delta x, y, z) - P(x, y, z))}{\Delta x}$$

Expanding $P(x + \Delta x, y, z)$ about x using Taylor Series we get:

$$P(x + \Delta x, y, z) = P(x, y, z) + \left. \frac{\Delta P}{\Delta x} \right|_x \Delta x + ..$$

Therefore the force due to pressure per unit volume at any point inside the channel may be written as

$$F_{\text{Pressure}} = \frac{(P(x + \Delta x) - P(x))}{\Delta x} \sim \frac{\Delta P}{\Delta x}$$

In the similar manner, if we consider the entire channel of length L and the pressure at input to be P_{in} and the pressure at the output to be P_{out} , then the force per unit volume may be written as

$$F_{\text{Pressure}} = \frac{P_{\text{out}} - P_{\text{in}}}{L} = \frac{\Delta P}{L} \quad (30)$$

For flow to happen from input to output, ΔP should be negative.

Viscous force acting on the liquid per unit volume may be calculated by considering a volume element in either the top or bottom portion with respect to the center of symmetry of the micro-channel (see figure 7.2).

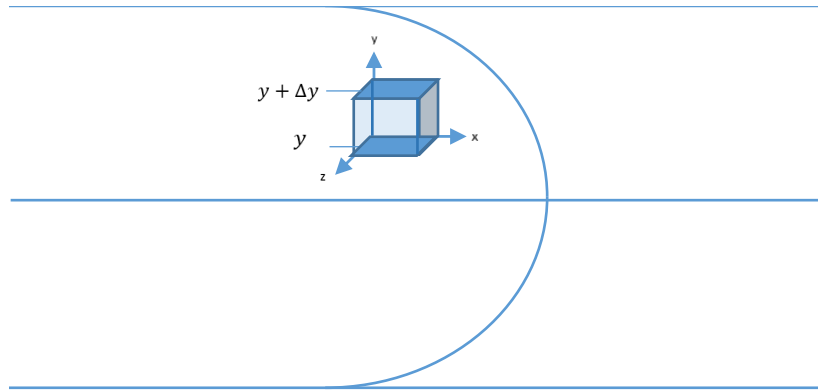


Figure 7.2 Positioning of the Volume Element in the Channel

Velocity of the liquid on the top surface of the volume element will be less than the velocity of the liquid on the bottom surface. The unequal viscous force on both the surfaces of the element will result in the shear of the liquid element.

The viscous force per unit area on the top surface may be written as:

$$\frac{F_{\text{Viscous}}^{\text{Top}}}{dA} = -\mu \left. \frac{dv_x}{dy} \right|_{y+\Delta y}$$

This force seems to move the liquid along the left.

Similarly, the viscous force per unit area on the bottom surface may be written as

$$\frac{F_{\text{Viscous}}^{\text{Bottom}}}{dA} = \mu \left. \frac{dv_x}{dy} \right|_y$$

This force seems to move the liquid towards the right

Therefore the net viscous force per unit area on the volume element may be written as

$$\frac{F_{\text{net}}}{dA} = \mu \left[\left. \frac{dv_x}{dy} \right|_y - \left. \frac{dv_x}{dy} \right|_{y+\Delta y} \right]$$

$$F_{\text{net}} = \mu dA \left[\left. \frac{dv_x}{dy} \right|_y - \left. \frac{dv_x}{dy} \right|_{y+\Delta y} \right]$$

Viscous force per unit volume becomes

$$F_{\text{Viscous}} = \frac{F_{\text{net}}}{dV} = \frac{F_{\text{net}}}{dA \Delta y} = -\frac{\mu}{\Delta y} \left[\left. \frac{dv_x}{dy} \right|_{y+\Delta y} - \left. \frac{dv_x}{dy} \right|_y \right]$$

$$= -\mu \left[\frac{\left. \frac{dv_x}{dy} \right|_{y+\Delta y} - \left. \frac{dv_x}{dy} \right|_y}{\Delta y} \right]$$

Expanding $\left. \frac{dv_x}{dy} \right|_{y+\Delta y}$ about y using Taylor Series we get

$$\left. \frac{dv_x}{dy} \right|_{y+\Delta y} = \left. \frac{dv_x}{dy} \right|_y + \left. \frac{d^2 v_x}{dy^2} \right|_y \Delta y + \dots$$

The viscous force per unit volume can be given as

$$F_{\text{Viscous}} = -\mu \frac{d^2 v_x}{dy^2} \quad (31)$$

In steady state (when force due to pressure is balanced by the viscous force), the liquid moves with constant velocity. In such a case, we should have:

$$\rho \frac{dv}{dt} = 0$$

Therefore eq. 3 becomes

$$F_{\text{Pressure}} + F_{\text{Viscous}} = 0 \quad (32)$$

Substituting eq. 4 and 5 in 6, we get

$$\frac{\Delta P}{L} - \mu \frac{d^2 v_x}{dy^2} = 0$$

$$\mu \frac{d^2 v_x}{dy^2} = \frac{\Delta P}{L} \quad (33)$$

Upon double integration of eq. 7 we get

$$v_x = \frac{\Delta P}{\mu L} \left(\frac{y^2}{2} \right) + C_1 y + C_2 \quad (34)$$

Applying the boundary conditions for a liquid flowing inside a channel, we get

1. At $y = 0$, $\frac{dv_x}{dy} = 0$. Substituting this in eq. 8, we get

$$0 = 0 + C_1$$

$$C_1 = 0$$

2. At $y = w$, $v_x = 0$ (No-slip condition), where w is half width of the channel.

Substituting this in eq. 8, we get

$$0 = \frac{\Delta P}{\mu L} \left(\frac{w^2}{2} \right) + 0 + C_2$$

$$C_2 = -\frac{\Delta P}{\mu L} \left(\frac{w^2}{2} \right)$$

Finally, substituting the values of C_1 and C_2 in eq. 8, we get

$$v_x = \frac{\Delta P}{\mu L} \left(\frac{y^2}{2} \right) - \frac{\Delta P}{\mu L} \left(\frac{w^2}{2} \right)$$

$$v_x = \frac{\Delta P}{2\mu L} (y^2 - w^2)$$

Therefore,

$$\mu = \frac{w^2 \Delta P}{2v_x L} \left(\frac{y^2}{w^2} - 1 \right) \quad (35)$$

where

μ is the viscosity of the liquid flowing in the channel

w is the half width of the channel

ΔP is the Pressure differential between the inlet and outlet ports v_x is the velocity of the liquid flowing inside the channel

L is the length of the channel

8. REFERENCES

- [1] J. V. Patton, "Ceramic magnet motor," ed: Google Patents, 1991.
- [2] M. Takara, "Electromagnetic piston engine," ed: Google Patents, 2000.
- [3] G. S. Bisht, S. Holmberg, L. Kulinsky, and M. Madou, "Diffusion-Free Mediator Based Miniature Biofuel Cell Anode Fabricated on a Carbon-MEMS Electrode," *Langmuir*, vol. 28, pp. 14055-14064, 2012.
- [4] L. C. Capretto, Wei; Hill, Martyn; Zhang, Xunli, "Micromixing within microfluidic devices," in *Microfluidics*, ed: Springer, 2011, pp. 27-68.
- [5] C.-C. Chang and R.-J. Yang, "Electrokinetic mixing in microfluidic systems," *Microfluidics and Nanofluidics*, vol. 3, pp. 501-525, 2007.
- [6] J. A. Chevalier, F., "Microfluidic on chip viscometers," *Review of Scientific Instruments*, vol. 79, pp. -, 2008.
- [7] D. P. Ciceri, Jilka M; Stevens, Geoffrey W, "A study of molecular diffusion across a water/oil interface in a Y-Y shaped microfluidic device," *Microfluidics and Nanofluidics*, vol. 11, pp. 593-600, 2011.
- [8] J. A. Kinast, "Production of Biodiesels from Multiple Feedstocks and Properties of Biodiesels and Biodiesel/Diesel Blends," National Renewable Energy Laboratory, Colorado, Report NREL/SR-510-31460, 2003/03 2003.
- [9] B. Ghosh, S. K. Haldar, and A. Nag, "Synthesis of Biodiesel from Oils of Jatropha, Karanja and Putranjiva to utilize in Ricardo Engine and its Performance & Emission Measurement," in *4th BSME-ASME International Conference on Thermal Engineering, December, 2008*, pp. 27-29.
- [10] G. S. Knothe, K. R., "Kinematic viscosity of biodiesel fuel components and related compounds. Influence of compound structure and comparison to petrodiesel fuel components," *Fuel*, vol. 84, pp. 1059-1065, 2005.
- [11] S. R. Yadav, V. K. Murthy, D. Mishra, and B. Baral, "Estimation of petrol and diesel adulteration with kerosene and assessment of usefulness of selected automobile fuel quality test parameters," *International Journal of Environmental Science & Technology*, vol. 1, pp. 253-255, 2005/12/01 2005.
- [12] T. Kobayashi and S. Konishi, "Microfluidic chip with serially connected filters for improvement of collection efficiency in blood plasma separation," *Sensors and Actuators B: Chemical*, vol. 161, pp. 1176-1183, 2012.
- [13] M. Sun, G. Velve Casquillas, S. Guo, J. Shi, H. Ji, Q. Ouyang, and Y. Chen, "Characterization of microfluidic fuel cell based on multiple laminar flow," *Microelectronic Engineering*, vol. 84, pp. 1182-1185, 2007.
- [14] J. W. Weaver, *Composition and behavior of fuel ethanol*: US Environmental Protection Agency, Office of Research and Development, 2009.

- [15] P.-C. P. Chen, Chang-Wei; Lee, Wei-Chen; Li, Kuan-Ming, "Optimization of micromilling microchannels on a polycarbonate substrate," *International Journal of Precision Engineering and Manufacturing*, vol. 15, pp. 149-154, 2014/01/01 2014.
- [16] S. Goel, P. Venkateswaran, R. Prajesh, and A. Agarwal, "Rapid and automated measurement of biofuel blending using a microfluidic viscometer," *Fuel*, 2014.
- [17] P. Commission, "Report of the committee on development of bio-fuel," 2003.
- [18] P. A. Studer, "Linear magnetic motor/generator," ed: Google Patents, 1982.
- [19] M. Gattani, "Design and Development of Linear Magnetic Generator," 1963.
- [20] B. V. Shenoy, "Lessons learned from attempts to reform India's kerosene subsidy," *Available at SSRN 1573587*, 2010.
- [21] A. Gupta and R. Sharma, *A new method for estimation of automobile fuel adulteration*: INTECH Open Access Publisher, 2010.
- [22] M. G. Badami, "Transport and urban air pollution in India," *Environmental Management*, vol. 36, pp. 195-204, 2005.
- [23] J. Gruber, A. R. Benvenho, R. Lippi, and R. W. Li, *Analytical Methods for Determining Automotive Fuel Composition*: INTECH Open Access Publisher, 2011.
- [24] P. Banerjee, U. Salunkhe, and S. Ravishankar, "Development of Vehicular Fuel Efficiency Norms and Labeling in India-Uniqueness of Challenging Scenario," SAE Technical Paper2009.
- [25] S. Roy, "Fiber optic sensor for determining adulteration of petrol and diesel by kerosene," *Sensors and Actuators B: Chemical*, vol. 55, pp. 212-216, 1999.
- [26] V. Mishra, S. C. Jain, N. Singh, G. Poddar, and P. Kapur, "Fuel adulteration detection using long period fiber grating sensor technology," *Journal of Scientific and Industrial Research (JSIR)*, vol. 46, pp. 106-110, 2008.
- [27] R. W. Li, L. R. Carvalho, L. Ventura, and J. Gruber, "Low cost selective sensor for carbonyl compounds in air based on a novel conductive poly (p-xylylene) derivative," *Materials Science and Engineering: C*, vol. 29, pp. 426-429, 2009.
- [28] A. R. Benvenho, R. W. Li, and J. Gruber, "Polymeric electronic gas sensor for determining alcohol content in automotive fuels," *Sensors and Actuators B: Chemical*, vol. 136, pp. 173-176, 2009.
- [29] X. J. Li, S. J. Chen, and C. Y. Feng, "Characterization of silicon nanoporous pillar array as room-temperature capacitive ethanol gas sensor," *Sensors and Actuators B: Chemical*, vol. 123, pp. 461-465, 2007.
- [30] N. K. L. Wiziack, A. Catini, M. Santonico, A. D'amico, R. Paolesse, L. Paterno, F. J. Fonseca, and C. Di Natale, "A sensor array based on mass

- and capacitance transducers for the detection of adulterated gasolines," *Sensors and Actuators B: Chemical*, vol. 140, pp. 508-513, 2009.
- [31] N. Srivastava and M. A. Burns, "Electronic drop sensing in microfluidic devices: automated operation of a nanoliter viscometer," *Lab on a Chip*, vol. 6, pp. 744-751, 2006.
- [32] J. Lee and A. Tripathi, "Intrinsic Viscosity of Polymers and Biopolymers Measured by Microchip," *Analytical Chemistry*, vol. 77, pp. 7137-7147, 2005/11/01 2005.
- [33] J. Chevalier and F. Ayela, "Microfluidic on chip viscometers," *Review of Scientific Instruments*, vol. 79, p. 076102, 2008.
- [34] Z. Han, X. Tang, and B. Zheng, "A PDMS viscometer for microliter Newtonian fluid," *Journal of Micromechanics and Microengineering*, vol. 17, p. 1828, 2007.
- [35] Z. Han and B. Zheng, "A poly (dimethylsiloxane) viscometer for microliter power law fluids," *Journal of Micromechanics and Microengineering*, vol. 19, p. 115005, 2009.
- [36] R. Bird, W. E. Stewart, and E. N. Lightfoot, "Transport Phenomena. Second," *J. Wiley*, 2002.
- [37] B. Bhushan, *Springer handbook of nanotechnology*: Springer Science & Business Media, 2010.
- [38] T. J. Snyder, M. Andrews, M. Weislogel, P. Moeck, J. Stone-Sundberg, D. Birkes, M. P. Hoffert, A. Lindeman, J. Morrill, O. Fercak, S. Friedman, J. Gunderson, A. Ha, J. McCollister, Y. Chen, J. Geile, A. Wollman, B. Attari, N. Botnen, V. Vuppuluri, J. Shim, W. Kaminsky, D. Adams, and J. Graft, "3D Systems' Technology Overview and New Applications in Manufacturing, Engineering, Science, and Education," *3D Printing and Additive Manufacturing*, vol. 1, pp. 169-176, 2014/09/01 2014.
- [39] apos, P. F. Neill, A. Ben Azouz, M. Vázquez, J. Liu, S. Marczak, Z. Slouka, H. C. Chang, D. Diamond, and D. Brabazon, "Advances in three-dimensional rapid prototyping of microfluidic devices for biological applications," *Biomicrofluidics*, vol. 8, p. 052112, 2014.
- [40] S. Begolo, D. V. Zhukov, D. A. Selck, L. Li, and R. F. Ismagilov, "The pumping lid: investigating multi-material 3D printing for equipment-free, programmable generation of positive and negative pressures for microfluidic applications," *Lab on a Chip*, vol. 14, pp. 4616-4628, 2014.
- [41] D. J. Beebe, G. A. Mensing, and G. M. Walker, "Physics and Applications of Microfluidics in Biology," *Annual Review of Biomedical Engineering*, vol. 4, pp. 261-286, 2002.
- [42] G. S. Fiorini and D. T. Chiu, "Disposable microfluidic devices: fabrication, function, and application," *BioTechniques*, vol. 38, pp. 429-446, 2005.
- [43] D. Kashyap, P. K. Dwivedi, J. K. Pandey, Y. H. Kim, G. M. Kim, A. Sharma, and S. Goel, "Application of electrochemical impedance spectroscopy in bio-fuel cell characterization: A review," *International journal of hydrogen energy*, vol. 39, pp. 20159-20170, 2014.

- [44] M. Santhiago and L. T. Kubota, "A new approach for paper-based analytical devices with electrochemical detection based on graphite pencil electrodes," *Sensors and Actuators B: Chemical*, vol. 177, pp. 224-230, 2013.
- [45] S. Xiong, A. Liu, L. Chin, and Y. Yang, "An optofluidic prism tuned by two laminar flows," *Lab on a Chip*, vol. 11, pp. 1864-1869, 2011.
- [46] K. B. Anderson, S. Y. Lockwood, R. S. Martin, and D. M. Spence, "A 3D Printed Fluidic Device that Enables Integrated Features," *Analytical Chemistry*, vol. 85, pp. 5622-5626, 2013/06/18 2013.
- [47] P. N. Nge, C. I. Rogers, and A. T. Woolley, "Advances in Microfluidic Materials, Functions, Integration, and Applications," *Chemical Reviews*, vol. 113, pp. 2550-2583, 2013/04/10 2013.
- [48] L. Wang, R. Kodzius, X. Yi, S. Li, Y. S. Hui, and W. Wen, "Prototyping chips in minutes: Direct Laser Plotting (DLP) of functional microfluidic structures," *Sensors and Actuators B: Chemical*, vol. 168, pp. 214-222, 2012.
- [49] C.-W. K. Park, Kye-Si; Kim, Wook-Bae; Min, Byung-Kwon; Park, Sung-Jun; Sung, In-Ha; Yoon, YoungSik; Lee, Kyung-Soo; Lee, Jong-Hang; Seok, Jongwon, "Energy consumption reduction technology in manufacturing — A selective review of policies, standards, and research," *International Journal of Precision Engineering and Manufacturing*, vol. 10, pp. 151-173, 2009/12/01 2009.
- [50] S. H. Y. Park, In Mo; Lim, Yunsung; Lee, Chang Sik, "Influence of the mixture of gasoline and diesel fuels on droplet atomization, combustion, and exhaust emission characteristics in a compression ignition engine," *Fuel Processing Technology*, vol. 106, pp. 392-401, 2013.
- [51] Y.-H. L. Seo, Hyun-Min; Jeon, Sang-Kwang; Ku, Tae-Wan; Kang, Beom-Soo; Kim, Jeong, "Homogenization of dimpled tube and its application to structural integrity evaluation for a dimple-type EGR cooler using FEM," *International Journal of Precision Engineering and Manufacturing*, vol. 13, pp. 183-191, 2012/02/01 2012.
- [52] S. P. Raju, Shinoj; Chand, Ramesh; Joshi, PK; Kumar, Praduman; Msangi, Siwa, "Biofuels in India: Potential, Policy and Emerging Paradigms-Vijaya Venkatesh," *Indian Journal of Agricultural Economics*, vol. 67, p. 268, 2012.
- [53] T. J. Vilknor, Dirk; Manz, Andreas, "Micro Total Analysis Systems. Recent Developments," *Analytical Chemistry*, vol. 76, pp. 3373-3386, 2004/06/01 2004.
- [54] K. Y. Ichihashi, Dai; Kurokawa, Hiroshi; Igarashi, Akinori; Yajima, Toshio; Fujiwara, Masami; Maeno, Katsuhiro; Sekiguchi, Shizuo; Iwata, Mitsuo; Nishino, Hoyoku, "Dynamic Analysis of Phorbol Esters in the Manufacturing Process of Fatty Acid Methyl Esters from *Jatropha curcas* Seed Oil," *Journal of the American Oil Chemists' Society*, vol. 88, pp. 851-861, 2011/06/01 2011.

- [55] S. H. L. Park, Chang Sik, "Combustion performance and emission reduction characteristics of automotive DME engine system," *Progress in Energy and Combustion Science*, vol. 39, pp. 147-168, 2013.
- [56] S. H. L. Park, Chang Sik; Yoon, Seung Hyun; Lee, Chang Sik, "HC and CO emissions reduction by early injection strategy in a bioethanol blended diesel-fueled engine with a narrow angle injection system," *Applied Energy*, vol. 107, pp. 81-88, 2013.
- [57] J. B. Atencia, David J, "Controlled microfluidic interfaces," *Nature*, vol. 437, p. 8, 2005.
- [58] S. C. Kumar, Alok; Jain, Shashi Kumar, "Critical review of jatropha biodiesel promotion policies in India," *Energy Policy*, vol. 41, pp. 775-781, 2012.
- [59] J. R. Benemann, "Chemicals and fuels from semi-arid zone biomass," in *The Biosaline Concept*, ed: Springer, 1979, pp. 309-331.
- [60] H. B. Zuoyan, Zheng, "A poly(dimethylsiloxane) viscometer for microliter power law fluids," *Journal of Micromechanics and Microengineering*, vol. 19, p. 115005, 2009.
- [61] H. X. Zuoyan, Tang; Bo, Zheng, "A PDMS viscometer for microliter Newtonian fluid," *Journal of Micromechanics and Microengineering*, vol. 17, p. 1828, 2007.
- [62] J. T. Lee, Anubhav, "Intrinsic Viscosity of Polymers and Biopolymers Measured by Microchip," *Analytical Chemistry*, vol. 77, pp. 7137-7147, 2005/11/01 2005.
- [63] C.-Y. T. Sue, Nan-Chyuan, "Human powered MEMS-based energy harvest devices," *Applied Energy*, vol. 93, pp. 390-403, 2012.
- [64] J. Topolnicki, M. Kudasik, N. Skoczylas, and J. Sobczyk, "Low cost capillary flow meter," *Sensors and Actuators A: Physical*, vol. 152, pp. 146-150, 2009.
- [65] S. Goel, *Opto-biochips for Microcytometry*: University of Alberta-Dept. of Electrical and Computer Engineering, 2006.
- [66] N. B. Srivastava, Mark A., "Electronic drop sensing in microfluidic devices: automated operation of a nanoliter viscometer," *Lab on a Chip*, vol. 6, pp. 744-751, 2006.
- [67] O. A. Skurtys, JM, "Applications of microfluidic devices in food engineering," *Food Biophysics*, vol. 3, pp. 1-15, 2008.
- [68] M. S. Y. El-Genk, In-Hwan, "Numerical analysis of laminar flow in micro-tubes with a slip boundary," *Energy Conversion and Management*, vol. 50, pp. 1481-1490, 2009.
- [69] M. Gorji, M. Alipanah, M. Shateri, and E. Farnad, "Analytical solution for laminar flow through leaky tube," *Applied Mathematics and Mechanics*, vol. 32, pp. 69-74, 2011.
- [70] E. d. R. Verpoorte, N. F., "Microfluidics meets MEMS," *Proceedings of the IEEE*, vol. 91, pp. 930-953, 2003.
- [71] J. L. Xuan, Michael K. H.; Leung, Dennis Y. C.; Wang, Huizhi, "Towards orientation-independent performance of membraneless microfluidic fuel

- cell: Understanding the gravity effects," *Applied Energy*, vol. 90, pp. 80-86, 2012.
- [72] A. M. Rasmussen, C.; Zaghoul, M. E.; Mikulchenko, O.; Mayaram, K., "Simulation and optimization of a microfluidic flow sensor," *Sensors and Actuators A: Physical*, vol. 88, pp. 121-132, 2001.
- [73] P. Venkateswaran, D. Kashyap, A. Agarwal, and S. Goel, "Computational Analysis of a Microfluidic Viscometer and Its Application in the Rapid and Automated Measurement of Biodiesel Blending Under Pressure Driven Flow," *Journal of Computational and Theoretical Nanoscience*, vol. 12, pp. 2311-2317, 2015.
- [74] A. H. Abdallah, Martin; Jakoby, Bernhard, "Measurement error estimation and quality factor improvement of an electrodynamic-acoustic resonator sensor for viscosity measurement," *Sensors and Actuators A: Physical*, vol. 199, pp. 318-324, 2013.
- [75] K. Dutkowski, "Experimental investigations of Poiseuille number laminar flow of water and air in minichannels," *International Journal of Heat and Mass Transfer*, vol. 51, pp. 5983-5990, 2008.
- [76] A. S. Wiley, "Milk for "Growth": Global and Local Meanings of Milk Consumption in China, India, and the United States," *Food and Foodways*, vol. 19, pp. 11-33, 2011.
- [77] A. Kumar, P. Joshi, P. Kumar, and S. Parappurathu, "Trends in the consumption of milk and milk products in India: implications for self-sufficiency in milk production," *Food Security*, vol. 6, pp. 719-726, 2014.
- [78] B.-B. A. H. Statistics, "Department of Animal Husbandry, Dairying & Fisheries, Ministry of Agriculture, Government of India," *KrishiBhavan, New Delhi*, 2012.
- [79] S. Lingathurai and P. Vellathurai, "Bacteriological quality and safety of raw cow milk in Madurai, South India," 2010.
- [80] J. Breman, *Patronage and exploitation: changing agrarian relations in south Gujarat, India*: Univ of California Press, 1974.
- [81] S. Roy and D. Rangnekar, "Farmer Participatory Need-based Extension (FPNE) approach: a sustainable model adopted by cooperative milk unions in Andhra Pradesh, India," *Livestock Research for Rural Development*, vol. 19, 2007.
- [82] G. Myrdal, "Corruption as a hindrance to modernization in South Asia," *Political Corruption: A Handbook*, ed. Arnold J. Heidenheimer, Michael Johnston, and Victor T. Le Vine (New Brunswick, NJ: Transaction Books, 1989), pp. 265-79, 1968.
- [83] L. Samal and A. Pattanaik, "Dairy Production in India-Existing Scenario and Future Prospects," *International Journal of Livestock Research*, vol. 4, pp. 105-113, 2014.
- [84] R. Chakravarty, "IT at Milk Collection Centers in Cooperative Diaries: The National Dairy Development Board Experience," *Information and Communication Technology in Development: Cases from India*, Sage Publications, India, 2000.

- [85] G. H. Richardson, "Automated Testing of Milk," *Journal of Dairy Science*, vol. 64, pp. 1087-1095, 1981.
- [86] A. Sadat, P. Mustajab, and I. A. Khan, "Determining the adulteration of natural milk with synthetic milk using ac conductance measurement," *Journal of Food Engineering*, vol. 77, pp. 472-477, 2006.
- [87] M. Sharifi and B. Young, "Towards an online milk concentration sensor using ERT: Correlation of conductivity, temperature and composition," *Journal of Food Engineering*, vol. 116, pp. 86-96, 2013.
- [88] M. Kozempel, "Viscosity and Density of Lactulose Solutions," *Journal of Dairy Science*, vol. 79, pp. 2152-2154, 1996.
- [89] T. Shellhammer, T. Rumsey, and J. Krochta, "Viscoelastic properties of edible lipids," *Journal of Food Engineering*, vol. 33, pp. 305-320, 1997.
- [90] L. M. Reid, C. P. O'Donnell, and G. Downey, "Recent technological advances for the determination of food authenticity," *Trends in Food Science & Technology*, vol. 17, pp. 344-353, 2006.
- [91] M. Martínez, "Hagen-Poiseuille Flow Solutions in Grad-Type Equations," *Journal of Statistical Physics*, vol. 142, pp. 710-725, 2011.
- [92] O. Paydar, C. Paredes, Y. Hwang, J. Paz, N. Shah, and R. Candler, "Characterization of 3D-printed microfluidic chip interconnects with integrated O-rings," *Sensors and Actuators A: Physical*, vol. 205, pp. 199-203, 2014.
- [93] T. F. Holden, N. C. Aceto, and E. F. Schoppet, "Effects of Viscosity and Temperature on the Foaming Characteristics of Concentrated Whole Milk," *Journal of Dairy Science*, vol. 47, pp. 359-364, 1964.
- [94] S. Kasemsumran, W. Thanapase, and A. Kiatsoonthon, "Feasibility of near-infrared spectroscopy to detect and to quantify adulterants in cow milk," *Analytical Sciences*, vol. 23, p. 907, 2007.
- [95] M. Ayub, Q. Ahmad, M. Abbas, I. M. Qazi, and I. A. Khattak, "Composition and adulteration analysis of milk samples," *Sarhad Journal of Agriculture*, vol. 23, p. 1127, 2007.
- [96] S. K. Nayak, A. Makrariya, R. R. B. Singh, A. A. Patel, J. S. Sindhu, G. R. Patil, and P. Tomar, "Heat stability and flow behaviour of buffalo milk added with corn starch," *Food Hydrocolloids*, vol. 18, pp. 379-386, 2004.
- [97] N. Silalai and Y. H. Roos, "Mechanical relaxation times as indicators of stickiness in skim milk-maltodextrin solids systems," *Journal of Food Engineering*, vol. 106, pp. 306-317, 2011.
- [98] U. Trivedi, D. Lakshminarayana, I. Kothari, N. Patel, H. Kapse, K. Makhija, P. Patel, and C. Panchal, "Potentiometric biosensor for urea determination in milk," *Sensors and Actuators B: Chemical*, vol. 140, pp. 260-266, 2009.
- [99] G. K. Mishra, R. K. Mishra, and S. Bhand, "Flow injection analysis biosensor for urea analysis in adulterated milk using enzyme thermistor," *Biosensors and Bioelectronics*, vol. 26, pp. 1560-1564, 2010.
- [100] L. A. Dias, A. M. Peres, A. C. Veloso, F. Reis, M. Vilas-Boas, and A. A. Machado, "An electronic tongue taste evaluation: Identification of goat

- milk adulteration with bovine milk," *Sensors and Actuators B: Chemical*, vol. 136, pp. 209-217, 2009.
- [101] W. S. Fyfe, N. J. Price, and A. B. Thompson, *Fluids in the Earth's Crust* vol. 383: Elsevier Amsterdam, 1978.
- [102] K. H. Hentschel, "The influence of molecular structure on the frictional behaviour of lubricating fluids," *Journal of Synthetic Lubrication*, vol. 2, pp. 143-165, 1985.
- [103] E. W. Lemmon and R. Span, "Short fundamental equations of state for 20 industrial fluids," *Journal of Chemical & Engineering Data*, vol. 51, pp. 785-850, 2006.
- [104] S. Z. Erhan and J. M. Perez, *Biobased industrial fluids and lubricants*: AOCS Press, 2002.
- [105] S. L. Outcalt and M. O. McLinden, "Automated densimeter for the rapid characterization of industrial fluids," *Industrial & Engineering Chemistry Research*, vol. 46, pp. 8264-8269, 2007.
- [106] O. Ashour, C. A. Rogers, and W. Kordonsky, "Magnetorheological fluids: materials, characterization, and devices," *Journal of intelligent material systems and structures*, pp. 123-130, 1996.
- [107] A. Agoston, C. Ötsch, and B. Jakoby, "Viscosity sensors for engine oil condition monitoring—Application and interpretation of results," *Sensors and Actuators A: Physical*, vol. 121, pp. 327-332, 2005.
- [108] G. E. Totten, *Handbook of hydraulic fluid technology*: CRC Press, 2011.

9. BIO-DATA OF CANDIDATE

Venkateswaran P S, M.Tech, B.E

Contact: +91-7895734999 / Email: eashwarps@gmail.com

PROFESSIONAL EXPERIENCE

- July 2015 - Present **Senior Research Scientist**
Research and Development Department-Office of the Chancellor
University of Petroleum and Energy Studies
Laureate International Universities Network
Dehradun, India 248007
- June 2012 - June 2015 **Research Scientist**
Research and Development Department-Office of the Chancellor
University of Petroleum and Energy Studies
Laureate International Universities Network
Dehradun, India 248007
- Oct' 2011 - May 2012 **Doctoral Research Fellow**
Australian Institute for Bioengineering and Nanotechnology
University of Queensland
Brisbane, Australia 4072

EDUCATION

- 2009 – 2011 **M.Tech** - Anna University, Chennai, India
Major: Nanoscience and Technology (Materials Stream)
Thesis: Synthesis and Characterization of Graphene and its Application in Energy Systems (Hydrogen Production Chamber)
Advisor: R Jayavel, PhD, M.Phil.
Award: University First - Gold Medal (9.5/10.0 CGPA)
- 2005 - 2009 **B.E** - Anna University, Chennai, India
Major: Electronics and Communication (Wireless Systems)
Thesis: Air Mouse

Advisor: D Sheila, PhD, M.E., B.E.

Accomplishment: First Class with Distinction (80.80%).

2004 – 2005 **Higher Secondary** - St Mary's MBHS School at Chennai, India

Major: Science

Accomplishment: First Class with Distinction (96.25%)

2002 - 2003 **Grade X** - St Mary's MBHS School at Chennai, India

Major: General

Accomplishment: First Class with Distinction (90.00%)

OTHER ACADEMIC POSITIONS

Position	Programme	Period	Institution (s) Involved	Tasks
Chief Organizer	Innovate India-2014 Award Event and Conference	27-28 February 2014	National Research Development Council and University of Petroleum and Energy Studies, Dehradun India	Organization
Chief Organizer	First International Seminar on Nanotechnology in Conventional and Alternate Energy Systems: A Global Status and Pathway 2013	12-13 August 2013	University at Albany USA and University of Petroleum and Energy Studies, Dehradun India	Organization and Overseas Collaboration
Chief Organizer	NANOMEET 2010 National Level Technical Meet on Nanoscience and Technology	26-27 March 2010	Anna University Chennai India	Organization and Overseas Collaboration
Chief Organizer	YASHAS 2008 National Level	Spring 2008	Tagore Engineering	Organization and

	Techno- Management Meet		College, Anna University Chennai India	Sponsorship Facilitation
--	-------------------------------	--	--	-----------------------------

HONORS AND AWARDS

- 2015 **Development of the University (2014-15) - Letter of Appreciation**
Awarded by: Office of Management, University of Petroleum and Energy Studies.
- 2015 **Exemplary Research Facilitation-Certificate of Appreciation**
Awarded by: Office of Management, University of Petroleum and Energy Studies.
- 2015 **R&D C³ Research Award for Paper Publishing & Patent Application**
Awarded by: Bharat Ratna Professor C.N.R. Rao, FRS on behalf of UPES.
- 2014 **Research Coordination and Management (2013-14) - Letter of Appreciation**
Awarded by: Office of Management, University of Petroleum and Energy Studies.
- 2014 **R&D C³ Research Award for Patent Filing**
Awarded by: Office of Management, University of Petroleum and Energy Studies.
- 2012 **University of Queensland International Scholarship**
Awarded by: Graduate School, University of Queensland.
- 2011 **University Gold Medal for the Best Post-Graduate Student in Nanoscience**
Awarded by: Anna University, India.
- 2010 **Best Paper Presentation Award at National Conference on Nano-materials**
Awarded by Karunya University, Coimbatore India.
- 2009 **Graduate Stipend Award for GATE Score**
Awarded by: University Grants Commission, Government of India.

- 2009 **Student Council Chairman and Placement Coordinator-
Referee Letter**
Awarded by: Tagore Engineering College, Anna University,
Chennai-India.
- 2006 **College Second in Physics at the State Level University
Examinations**
Awarded by: Tagore Engineering College, Anna University,
Chennai India.
- 2004 **School First in the Grade XI Common Examination**
Awarded by: St Mary's MBHS School.
- 2003 **School First in History, Geography and Hindi Grade X State
Examination**
Awarded by: St Mary's MBHS School.

SPONSORED PROJECT COORDINATOR

- Fall 2014 – **Microfluidic Viscometer for Various Biochemical Applications**
Fall 2015 [Technology Systems Development Program](#)-Department of
Science and Technology-Government of India
PIs: Dr. Sanket Goel & Dr. Ajay Agarwal (CSIR-CEERI) | Value:
113, 000 US\$
- Spring 2013 – **Membrane-less Microfluidic devices for rapid, automated and**
Fall 2015 **Self-sustainable enzymatic biofuel cell with 3D electrodes for in
vivo and ex vivo devices**
[Indo-Korea Joint Research Project](#)-Department of Science and
Technology-Government of India
PIs: Dr. Sanket Goel and Dr. Gyu Man Kim | Value: 40, 300 US\$
- Fall 2013 – **Microfluidic Diffusivity Meter-CO2 diffusivity sensor during**
Fall 2015 **Carbon Sequestration in Oil Reservoirs**
[Young Scientist Program](#)-Department of Science and Technology-
Government of India
PI: Dr. Sanket Goel | Value: 35, 500 US\$

CERTIFICATIONS

- Fall 2012 **Semiconductor Technology and Manufacturing**
IIT Bombay and Applied Materials Inc., IIT Bombay
- Spring 2011 **International English Language Testing System**
Score: 8.0/9.0 [Ref. No.-10IN029250PEDS001A]

- Spring 2009 **All India GATE Examination**
Score: 94 Percentile
- Fall 2008 **ESOL International Business English Certificate**
Cambridge University ESOL, UK [Ref. No. - 089IN0010111]
- Fall 2008 **C++, Linux Power User and HTML Programming**
Certification from NIIT- India
- June 2007 **In-plant Training at Rajiv Gandhi Memorial Telecom
Training Centre**
Certification from Bharat Sanchar Nigam Ltd.

PATENTS AND PUBLICATIONS

PATENTS FILED

1. **Venkateswaran, P.S.**, Abhishek Sharma, Ajay Agarwal and Sanket Goel., An Optofluidic Microviscometer for measuring Adulteration in a Fluid– Filed at the New Delhi Patents Office – Patent Application No. - #780/DEL/2015.
2. Diwakar Kashyap, **Venkateswaran, P.S.**, Jitendra K. Pandey and Sanket Goel, Fabrication of Vertically aligned Copper Nanotubes (CuNTs) as a Novel Electrode for Enzymatic Biofuel Cells (EBFCs) – Filed at the New Delhi Patents Office – Patent Application No. - #122/DEL/2015.
3. Sanket Goel, **Venkateswaran, P.S.**, Ajay Agarwal and Rahul Prajesh, Micro-fluidic device (Micro Viscometer) and a method of determining viscosity thereon for detection and monitoring applications - Filed at the New Delhi Patents Office - Patent Application No. - #2713/DEL/2013.

PEER-REVIEWED JOURNAL ARTICLES

1. Sonal Singh, Shikha Jain, **Venkateswaran PS**, Avani K. Tiwari, Mansa R. Nouni, Jitendra K. Pandey, Sanket Goel, Hydrogen: A sustainable fuel for future of the transport sector, Renewable and Sustainable Energy Reviews, Volume 51, November 2015, Pages 623-633, ISSN 1364-0321, <http://dx.doi.org/10.1016/j.rser.2015.06.040>.
2. **P. S. Venkateswaran**, D. Kashyap, A. Agarwal, and S. Goel, "Computational Analysis of a Microfluidic Viscometer and Its Application in the Rapid and Automated Measurement of Biodiesel Blending Under

Pressure Driven Flow," Journal of Computational and Theoretical Nanoscience, vol. 12, pp. 2311-2317, 2015,
<http://dx.doi.org/10.1166/jctn.2015.4026>.

3. D. Kashyap, **P. S. Venkateswaran**, P. K. Dwivedi, Y. H. Kim, G. M. Kim, A. Sharma, and S. Goel, "Recent developments in enzymatic biofuel cell: towards implantable integrated micro-devices," International Journal of Nanoparticles, vol. 8, pp. 61-81, 2015,
<http://www.inderscienceonline.com/doi/abs/10.1504/IJNP.2015.070345>.
4. D. Kashyap, R. S. Yadav, S. Gohil, **P. S. Venkateswaran**, J. K. Pandey, G. M. Kim, Y. H. Kim, P. K. Dwivedi, A. Sharma, P. Ayyub, and S. Goel, "Fabrication of Vertically aligned Copper Nanotubes as a Novel Electrode for Enzymatic Biofuel Cells," Electrochimica Acta, vol. 167, pp. 213-218, 2015, <http://dx.doi.org/10.1016/j.electacta.2015.03.164>.
5. S. Goel, **P. Venkateswaran**, R. Prajesh, and A. Agarwal, "Rapid and automated measurement of biofuel blending using a microfluidic viscometer," Fuel, vol. 139, pp. 213-219, 2015,
<http://dx.doi.org/10.1016/j.fuel.2014.08.053>.
6. M. K. Gattani, **P. S. Venkateswaran**, P. K. Sahoo, and P. Diwan, "Dynamic Analysis of Gate Operated Magnetic Piston (GOPI) Engine Using ANSYS Software," 2014, vol. 7, 2014,
<http://dx.doi.org/10.15866/iremos.v7i6.4579>.
7. R. Yogamalar, **P. S. Venkateswaran**, M. R. Benzigar, K. Ariga, A. Vinu, and A. C. Bose, "Dopant Induced Bandgap Narrowing in Y-Doped Zinc Oxide Nanostructures," Journal of nanoscience and nanotechnology, vol. 12, pp. 75-83, 2012,
<http://dx.doi.org/10.1166/jnn.2012.5760>.

MANUSCRIPTS SUBMITTED FOR REVIEW

1. **P. S. Venkateswaran**, Abhishek Sharma, Ajay Agarwal and Sanket Goel, Rapid and Automated Measurement of Milk Adulteration using a 3D Printed Optofluidic MicroViscometer (OMV) - Sensors (IEEE), 2016.
2. Sanket Goel, Prabhat K Dwivedi, **P. S. Venkateswaran** and Ashutosh Sharma, Novel Fabrication Techniques for Integrated Microfluidic Devices for Energy, Environment and Biomedical Applications: A Review in Indian Scenario - Lab on Chip, 2016.

3. **P. S. Venkateswaran**, Abhishek Sharma, Ajay Agarwal and Sanket Goel, Rapid and Automated Measurement of Fuel Adulteration using a 3D Printed Optofluidic MicroViscometer (OMV) - Fuel, 2016.

CONFERENCE APPEARANCES

1. **Venkateswaran, P.S.**, Abhishek Sharma, Ajay Agarwal and Sanket Goel, Stereolithography (SLA) based 3D Printed Optofluidic MicroViscometer (OMV) for Rapid and Automated Measurement of Milk Adulteration, Indo-UK Workshop on Micro Nano Fluidics for Health & Diagnostics - [fluidicsHD - 2015](#), CSIR-CEERI, Pilani, August 27 - 28, 2015.
2. **Venkateswaran, P.S.**, Abhishek Sharma, Ajay Agarwal and Sanket Goel, 3D Printed Lab-on-a-chip Microviscometer for various Biochemical Applications, 15th IEEE International Conference on Environment and Electrical Engineering, Rome-Italy. 2015.
3. **Venkateswaran, P.S.**, Rahul Prajesh, Ajay Agarwal and Sanket Goel, [Rapid and Automated Measurement of Biofuel Blending using Microfluidic Device under Pressure Driven Flow using COMSOL Multiphysics](#), COMSOL Conference-Bangalore. 2013.
4. Sanket Goel, Deepak Rai, Paridhi Puri, Shivani Nain, Rahul Prajesh, **Venkateswaran, P.S.**, Ajay Agarwal, Rapid and Automated Measurement of Biofuel Blending using Microfluidic Device, International Conference on Sustainable Energy Technologies, Vancouver-Canada. 2012.
5. **Venkateswaran, P.S.**, Dushendra Babu and R Jayavel, Synthesis of Graphene and its Applications in Energy Systems, International Conference on Materials for the Future, Government Engineering College Trichur, Kerala India. February 2011.
6. **Venkateswaran, P.S.**, Dushendra Babu and R Jayavel, Synthesis of Graphitic Oxide and its Applications in Energy Systems and Nano-electronics, National Conference on Nano-materials, Karunya University, Coimbatore. 2010.

POSTER PRESENTATIONS

1. Akshaya Venkatakrishnan and **Venkateswaran P.S.**, Rapid Prototyping of Lab-on-chip Microfluidic Devices using Stereolithography (SLA) based 3D Printing, Bringing the Nanoworld Together 2015, Chennai-India.

2. **Venkateswaran, P.S.**, Nano-technological Advances in Drilling for Oil and Gas, Indo-Russian Round Table organized by “Russian-India Science and Technology Centre-Moscow-Russia” New Delhi-India. 2012.